The ICE-βox Integrative Conjugative Element of *Legionella pneumophila*

by

Kaitlin Jane Flynn

A dissertation submitted in partial fulfillment
of the requirements for the degree of
Doctor of Philosophy
(Microbiology and Immunology)
in The University of Michigan
2015

Doctoral committee:

Professor Michele S. Swanson, Chair
Professor Victor J. DiRita
Professor Harry L. T. Mobley
Associate Professor Lyle A. Simmons

“Somewhere, something incredible is waiting to be known.”

- Carl Sagan, Ph.D.

DEDICATION

For my mom, Karen

ACKNOWLEDGEMENTS

I have many wonderful people to thank for their support during my time in graduate school. First, I have tremendous respect and gratitude for my mentor, Michele. Michele has been an incredible professional and personal role model to me throughout my graduate career. She has taught me to think critically, to design careful and rigorous experiments and to write with clarity. Michele is an outstanding example of a wonderful scientist and mentor who balances her career with rich friendships, hobbies and a loving family. I have grown immensely as a scientist and as a young woman through Michele's guidance and I will always be grateful for her support. Michele has recruited a fantastic group of scientists to work with who have become like family over the years; I am particularly indebted to Brenda Byrne, our brilliant and kind technician. Brenda has taught me invaluable bench skills for the study of *Legionella* and cell-culture work and has always been eager to discuss data or experimental designs. Likewise, the senior graduate student Zack Abbott taught me the genetic techniques to manipulate and study *Legionella*. His energy, passion and creative thinking have been a great source of inspiration to my project. Over the years Zack has served as both a scientific advisor and best friend, and I am thankful to have trained alongside him.

I must also thank my thesis committee, Drs. Victor DiRita, Harry Mobley, John Moran and Lyle Simmons. These fantastic scientists came together to help develop my thesis project and pushed me to design rigorous experiments. Their range of expertise

and suggestions guided my thesis to completion. Outside of my committee, I'm thankful for the scientific guidance and advice offered by Drs. Paul Carlson, David Friedman, and Eric Martens.

My greatest sources of personal support and encouragement throughout my time in graduate school have been my best friends. My college friends Ashton Kunkle and Kyla Pitts-Zevin have always been my cheerleaders from afar and eagerly supported me in all of my endeavors. My first day at Michigan I met fellow graduate student Ariell Joiner, who has kept me sane by joining me for a run after work nearly every week for the last five years. Fellow microbiology graduate students Victoria Holden and Jay Lubow have been constant sources of scientific and emotional support, always available for lunch, a chat or a drink after work. Finally, in the last few months of completing my dissertation I had the fortune to meet the brilliant medical student Spencer Lewis. His drive, ambition, passion for science and medicine and commitment to personal growth has been a great source of inspiration and support. For my friends, I am forever thankful; I could not have finished this thesis without them beside me.

TABLE OF CONTENTS

DEDICATION……....ii

ACKNOWLEDGMENTS…….iii

LIST OF FIGURES…….....vii

LIST OF TABLES……..…….....viii

ABSTRACT…….....ix

CHAPTER ONE: INTRODUCTION……...1

Mobile Genetic Elements…….1
Integrative Conjugative Elements……..2
Phenotypic ICE Traits……..3
ICE Regulation……..5
Public Health Impact of ICEs……6
Legionella pneumophila Discovery and Epidemiology……...7
Legionella in the Environment……8
Intracellular Life Cycle of *L. pneumophila*……...10
L. pneumophila Genetic Diversity……13
ICEs in *L. pneumophila*……....14
Outline of the Thesis……..15

CHAPTER TWO: INTEGRATIVE CONJUGATIVE ELEMENT ICE-βOX CONFERS OXIDATIVE STRESS RESISTANCE TO *LEGIONELLA PNEUMOPHILA IN VITRO* AND IN MACROPHAGES……17

Summary……..17
Introduction……..18
Experimental Procedures……..19
Results……..25
Discussion……...38

CHAPTER THREE: CsrA PARALOG CsrT REGULATES CORE AND ACCESSORY GENOME TRAITS IN *LEGIONELLA PNEUMOPHILA*……..43

Summary……..43
Introduction……..44
Experimental Procedures……..47
Results……..71
Discussion……88

CHAPTER FOUR: DISCUSSION……93
ICE-βox Epidemiology……103

BIBLIOGRAPHY……..108

LIST OF FIGURES

1.1 *L. pneumophila in vivo* infection models in two genetically distinct mice……12

2.1 ICE-βox is a mobile genetic element……24

2.2 ICE-βox excision is not coordinated with growth phase……30

2.3 ICE-βox promotes oxidative stress survival……32

2.4 Oxidative stress has minimal effect on ICE-βox mobility……..34

2.5 ICE-βox confers protection to *Legionella* in resistant macrophages……...36

3.1 Relationship of CsrA paralogs and T4SSs……..76

3.2 Ectopic *csrT* expression reduces ICE-βox transfer……....77

3.3 Ectopic *csrT* expression represses oxidative stress resistance conferred by ICE-βox……80

3.4 CsrT inhibits replication in macrophages independent of NADPH oxidase……84

3.5 CsrT inhibits motility via a conserved mechanism……..87

LIST OF TABLES

2.1 Primers used in Chapter Two…….24

3.1 Strains, plasmids and primers used in Chapter Three……...50

3.2 CsrA paralogs in *Legionellae* ICEs……56

3.3 Summary of ICEs from Figure 3.1B……..……...61

4.1 ICE-βox prevalence in *L. pneumophila* isolates from the CDC……..107

ABSTRACT

Legionella pneumophila is an accidental human pathogen that causes the bacterial pneumonia Legionnaire's Disease. The bacteria are ubiquitous in freshwater environments and are spread by aerosolization of contaminated water from the built environment. Accessory traits carried on mobile genetic elements diversify the *L. pneumophila* and may contribute to persistence in stressful environments. One class of mobile elements are Integrative Conjugative Elements (ICEs) which encode cargo genes as well as type IV secretion system (T4SS) transfer apparatuses to direct their own transmission among a bacterial population. In this dissertation, I demonstrate that ICE-βox enhances *L. pneumophila* resistance to oxidative stresses encountered *in vitro* (such as bleach) and in macrophages. Specifically, this mobile element protects *L. pneumophila* from the toxic activities of the macrophage phagocyte oxidase. In addition to cargo genes predicted to repair oxidative damage, ICE-βox encodes a paralog of the master *L. pneumophila* life cycle regulator *csrA.* Bioinformatic analyses of 34 *L. pneumophila* ICE-associated T4SS reveals four families based on apparatus composition. Each T4SS family is genetically and phylogenetically linked with a distinct *csrA* paralog, suggesting functional interactions. Indeed, the ICE-βox *csrA* paralog *csrT* can repress ICE-βox traits as well as motility of the host bacterium. Finally, a preliminary epidemiologic survey identified ICE-βox in a majority of built environment *L. pneumophila* isolates. Accordingly, the hypothesis that chlorine-based disinfectants

enrich for ICE-βox and increase *L. pneumophila* resilience and virulence warrants testing. By understanding the fitness advantages, regulation and prevalence of ICE-βox, disinfection protocols can be designed to eradicate persistent *L. pneumophila* and reduce its risk to humans.

CHAPTER ONE

Introduction

Mobile Genetic Elements

Bacteria rapidly evolve by acquiring genetic material via natural transformation of free DNA encountered in the environment, bacteriophage transduction or bacterial conjugation. These processes, collectively known as horizontal gene transfer, allow bacteria to acquire new genetic information not directly inherited from the parent cell. Conjugation is the process of bacterial mating, allowing for transfer of genetic material from one cell to another through a multi-subunit sex pilus that forms a protected tube through which DNA is transferred. Conjugative DNA elements take advantage of this mechanism to speed their dispersion within a population of bacterial cells. These elements use an encoded type IV secretion system (T4SS) as a sex pilus for transfer.

Bacterial T4SS are broadly classified into conjugative, DNA uptake and effector-translocating systems (1). Within the conjugative family, four distinct classes of genetic structures emerge known as type F (fertility), P (pilus), I (icm) or GI (genomic island associated) (2). These structural types represent the majority of conjugative elements and are further classified by transfer apparatus genes (*tra, virB,* etc) (2). Bacteria typically maintain only one of each type of T4SS-carrying plasmid within the cell, as like

plasmids compete for the replication machinery during bacterial division. Therefore, two plasmidsof the same type are incompatible and are poorly maintained in the host clonal population. By encoding diverse T4SS, conjugative plasmids increase their likelihood of being maintained by bacterial cells that may already carry one or more types of plasmids.

Integrative Conjugative Elements

Integrative Conjugative Elements (ICEs) are one type of conjugative plasmid. These elements are often large and carry their own GI-T4SS and transposition enzymes to regulate transfer (3). ICEs can excise from a host chromosome, form an episome and induce their own replication and transfer to a recipient cell using the encoded T4SS pilus (4), (3). Excision of the ICE requires conservation of short direct repeat nucleotide sequences, called attachment sites, which align during recombination events and facilitate site-specific ICE mobility. Importantly, excision leaves one attachment site on the chromosome and one on the ICE, allowing for reintegration after excision events (2), (3).

Much of the enzymatic machinery directing these processes have phage origins, as phages use a similar attachment site recognition mechanism for integration. Particularly, the integrases necessary for recombination are typically tyrosine or serine recombinases classically carried by transposons and phages (5). Some ICEs also carry immunity proteins to regulate transfer and prevent acquisition of similar ICEs, akin to phage exclusivity (3, 6). Similarly, some ICEs use homologs of the lambda phage

repressor protein cI to regulate transfer (3). Despite these genetic similarities, ICEs are distinct from phages, as they are capable of conjugative transfer and typically do not encode functional structural proteins such as capsid or tail fibers.

While traditionally described bacteriophages and conjugative transposons have defined genetic features, other mobile genetic elements tend to be more mosaic in structure. ICEs typically carry components from phages, plasmids and transposons acquired from the horizontal gene pool (7). Since each of these mobilizable systems contain both shared and unique features, the classification of these elements is better thought of as a continuum (7). Swapping of recombination and mobilization modules as well as cargo traits contributes to the rapid evolution of new ICEs. The ancestry of such component swapping can be traced by examining the content of guanine and cytosine (G+C%) within a given element. G+C% is a measure of genome similarity, which typically differs between regions of the core chromosome and horizontally acquired elements (8). Indeed, examination of ICE components reflects a highly variable G+C% within an element, reflecting their multiple origins and dynamic evolution (9).

Phenotypic ICE Traits

Importantly, ICEs encode cargo genes that can provide phenotypic advantages to their host. These proteins typically enhance bacterial survival in environmental conditions that coordinate with the host species they inhabit. For instance, genes encoded on an ICE in the sewage-isolated *Pseudomonas knackmussii* provide the ability to degrade 3-chlorobenzoic acid, whereas another ICE in the plant symbiont

Mesorhizobium loti equips this bacterium to fix nitrogen (3). These ICE-encoded mechanisms, therefore, expand the capacity of these organisms to metabolize compounds frequently encountered in their natural habitats (3).

High frequencies of horizontal gene transfer have been observed in soil bacteria isolated from hazardous waste sites. Radionuclides and heavy metals pose a serious threat to soil microbes, but also exert selective pressures that increase the burden of resistant organisms (10). Indeed, mercury, nickel, copper and arsenic resistance, as well as radionuclide-reducing enzymes, have been found to transfer via ICEs between both culturable and unculturable soil community members in these waste sites (10). Accordingly, ICEs not only promote evolution of metal-resistant soil microbes, but also may contribute to their fitness in other environments. Indeed, genes for metal resistance are often carried along with antibiotic resistance genes on conjugative elements, as a primary mechanism of each is the detoxification of the intracellular environment by multidrug efflux pumps (10-12). Finally, some ICEs encode non-traditional virulence factors such as the PAPI-1 pathogencity island in *P. aeruginosa*. PAPI-1 carries a *cupD* operon that produces extracellular fimbriae important for biofilm formation, increasing their persistence in the host and environment (13).

The most well studied beneficial conjugative elements are those that confer antibiotic resistance. Many bacteria are able to mitigate the damaging effects of antibiotics through a variety of mechanisms, including biochemical modification of a drug target, export of the compound through efflux pumps, altering membrane permeability or direct inactivation of the drug (14, 15). Genetically, bacteria can acquire

resistance through two mechanisms, either through mutation or, more commonly, through horizontal gene transfer of resistance determinants by conjugative elements such as ICEs (14). Indeed, ICE-mediated antibiotic resistance has been described in many bacterial species including *Vibrio cholerae*, *Haemophilis influenzae*, *Enterrococcus faecalis, Streptococcus pyogenes, Staphylococcus aureus,* and *Escherichia coli* (3, 4, 8). This cohort of pathogens employs diverse mechanisms of antibiotic resistance, including general resistance strategies such as efflux pumps as well as antibiotic-specific mechanisms in which ICEs encode enzymes that target individual drugs. Additionally, many of these ICEs confer resistance to multiple drugs by encoding many systems on one composite plasmid, such as the ICE-SXT from *V. cholerae,* which resists six different types of antibiotics (16).

ICE Regulation

Because ICEs encode independent operons devoted to transfer, excision and cargo, their gene expression must be tightly regulated to ensure each component functions at the right time. The regulatory mechanisms of ICEs are as diverse as the elements themselves. Some ICEs, including ICE*clc* from *P. aeruginosa* and CTnDOT from *B. thetaiotaomicron*, apparently rely entirely on regulators carried on the ICE to control expression of transfer, excision and cargo traits (17, 18). Others, like ICE-SXT and ICEBs1 from *Bacillus subtilis*, respond to cues initiated by master regulators encoded on the core chromosome, such as the SOS response regulator RecA (16, 19). In most cases, ICE regulatory cascades are induced by environmental stimuli, such as

exposure to antibiotics or metabolites, concordant with the phenotypes conferred by the ICE (3). As mentioned earlier, some ICEs ensure ICE maintenance and transfer by using regulatory systems acquired from phages, including the immunity proteins ImmR/S and the cI repressor (3, 6). In the end, timely expression of specific ICE traits is typically achieved through multiple regulatory mechanisms.

Public Health Impact of ICEs

The emergence of highly virulent pathogens is a direct consequence of the self-sufficient transfer machines encoded by ICEs. ICEs can spread rapidly among complex polymicrobial communities, including the gut microbiota, multispecies biofilms, wastewater and soil (20-22). Any chemical stressors present in these environments (antibiotics, disinfectants, pesticides) will eventually select for resistant organisms. Many of the acquired resistance mechanisms map to ICEs, which can be induced to excise upon sensing the very stress they mitigate. Thus, anti-microbial treatments directly promote ICE transfer. The increased burden of stress resistance due to horizontal gene transfer is a serious threat to public health, as the chemicals used to treat patients or disinfect hospitals or water systems can instead enrich for more fit strains of the pathogens they are meant to eradicate (20, 23).

The best example of resistance spread by horizontal gene transfer is the overuse of antibiotics in agricultural settings. Antibiotics are frequently incorporated into feed to promote growth and for prophylactic treatment of livestock, often at high doses. These compounds are eventually excreted into the environment and subsequently contaminate

the nearby soil and water systems (20). Agricultural use of antibiotics presents two significant public health concerns. First, resistant pathogens can arise and/or survive in the animal itself; subsequently, these resistant pathogens can exchange genetic information in the natural environment (24). Indeed, multi-locus sequence typing analysis of tetracycline-resistant *Staphylococcus aureus* clonal complex CC398 isolated from humans and livestock showed that strains were highly likely to acquire resistance in the animal or farm environment and then later be isolated from a human infection (25). This genetic analysis also specifically linked the resistance to acquisition of mobile genetic elements (25). Similarly, use of tetracycline in aquaculture environments has been linked to the selection for tetracycline resistant pathogens subsequently isolated from nearby hospital water systems (23). It is clear that human introduction of stringent chemicals contributes to evolution of virulent pathogens via ICE-mediated mechanisms.

Legionella pneumophila Discovery and Epidemiology

In July of 1976, an epidemic of fever, chest pain and gastrointestinal symptoms broke out at a convention of the American Legion in Philadelphia, PA (26). Of 182 infected individuals, 147 (81%) were hospitalized and 29 (16%) died from this illness. Pneumonia symptoms were strongly associated with pre-existing conditions, old age and immunosuppression in patients (26). Illness also correlated with increased time spent in the lobby or directly outside of the hotel and linked to water exposure, consistent with an airborne or waterborne pathogen. Microbiological examination of sputum from patients revealed a previously uncharacterized Gram-negative bacillus

(27). Initial pathology did not resemble the effects of any known pathogen. This outbreak represented a frightening time in public health—an uncharacterized and poorly understood air and waterborne pathogenic bacterium had been identified, and this organism seemed able to persist in public spaces and infect humans with a relatively high fatality rate. The responsible microbe was later named *Legionella pneumophila*, or "lung-loving", and the subsequent pneumonia known as Legionnaire's Disease.

Since 1976, there have been a number of outbreaks of Legionnaire's Disease around the world, most often linked to contaminated water systems (28). *L. pneumophila* is now known to be a waterborne pathogen that is spread by aerosolization of contaminated water and subsequent inhalation by humans. While an uncommon source of community-acquired pneumonia, *L. pneumophila* remains a significant threat to hospitalized patients, as a primary risk factor for *L. pneumophila* infection is immunosuppression (29). Once infected, the case fatality rate for immunocompromised patients can be as high as 80% (28, 30). Epidemiologic surveys of hospital water systems suggest 63%-84% of hospitals are colonized with some form of *Legionella* (31), contributing directly to nosocomial infections.

Legionella **in the Environment**

Legionella spp. are ubiquitous in natural freshwater and soil environments as planktonic forms or living inside amoebae (32, 33). Thirteen freshwater amoebae species including *Acanthamoeba castellani* and *Hartmonella vermiformis* provide a replicative environment for *Legionella*. Indeed, amoebae have been co-isolated with

Legionella from water sources linked to disease outbreaks (34). Phagocytic amoebae provide a protected replication niche for the bacteria and also allow *L. pneumophila* to adapt to life in harsh environments upon exit, via activation of stringent response genes within vacuoles (35, 36). Indeed, *L. pneumophila* passaged through amoebae are more resistant to high temperatures, pH, disinfectants and osmolarity changes after passage than unpassaged cells (37, 38). Additionally, the exiting *L. pneumophila* are significantly more infectious in mammalian cells, suggesting that the amoebae induce a hypervirulent state in *L. pneumophila* (39). Amoebae can also form highly resistant cysts in response to environmental stresses and protect *L. pneumophila* from the extracellular environment (40). It has been hypothesized that the relationship between amoebae and *L. pneumophila* serves as intracellular "training", preparing the bacteria to infect phagocytic alveolar macrophages (34).

Once infected amoebae or free *Legionella* make their way from a freshwater source to a built environment, the bacteria can persist in multiple forms. In addition to providing a replication niche, amoebae also release small *Legionella*-containing vesicles that are particularly resistant to freezing and biocides (41). The pipes and surfaces that make up the extensive water systems within engineered structures provide ideal sites for the development of multispecies biofilms. Amoebae play a role in this system too—*L. pneumophila* that have passed through amoebae are more efficient at forming biofilms and producing extracellular polysaccharides (42). However, presence of amoebae is likely not required for *L. pneumophila* biofilms to form, since this microbe can form monospecies biofilms on a number of different plumbing surfaces including plastic or

steel pipes (30). Attachment is thought to be mediated by extracellular structures such as type IV pili (T4SS) and fimbriae (30). Within biofilms, *L. pneumophila* is especially resistant to disinfecting biocides (43).

Resistance to chemical disinfectants is a recurrent problem encountered when attempting to control or limit *L. pneumophila* outbreaks. Outbreaks have been linked to cooling towers, whirlpools, soil, baths, fountains, wastewater treatment plants, ice machines, and other mechanical devices (33). Most of these systems employ chlorine-based disinfectants to treat the source water. Interestingly, treatment of hospital water systems with chlorination protocols actually increased the burden of *Legionellae* in 209 sites in Paris (44). Similarly, in an analysis of the effects of chloramine treatment on microbial communities in drinking water, the prevalence of *Legionellae* rose as the exposure time lengthened. In contrast, several other members of the community were completely eliminated, indicating that *Legionella* is at least partially resistant to these chemicals (45). Between amoebae, cysts, biofilms and chemical resistance to biocides, eradication of *Legionella* from both natural and man-made environments can be a particularly difficult, though very important, endeavor.

Intracellular Life Cycle of *L. pneumophila*

Legionellae can exist in many different forms in the environment. However, once *L. pneumophila* enters a human alveolar macrophage, it primarily cycles between two forms, replicative and transmissive. Upon phagocytosis, the core *dot/icm* T4SS releases protein effectors into the host cell cytosol that inhibit trafficking of the *Legionella*

Containing Vacuole (LCV) to late endosomal compartments (46, 47). Once the bacterium establishes a replicative compartment, it divides until nutrients become limiting. In this replicative state, transmissive phase genes including those for motility, sodium resistance and cytotoxicity are repressed (48). Upon detection of limiting concentrations of amino acids or fatty acids by the ppGpp synthetase proteins RelA and SpoT, respectively, the alarmone (ppGpp) is produced. ppGpp indirectly relieves CsrA-mediated repression of transmissive phase genes via a LetA/S signaling cascade (48-52). These transmissive traits equip *L. pneumophila* to become cytotoxic and motile, equipping the progeny bacteria to exit the cell and infect a new host (53).

The inflammatory response to *L. pneumophila* infection has been deduced by infecting mouse macrophages from distinct genetic backgrounds (Figure 1.1). In healthy macrophages, *L. pneumophila* induces an inflammatory cell death known as pyroptosis (54). Upon entering a mouse macrophage, *L. pneumophila* flagellin contaminates the cell cytosol, presumably by leaking through the *dot/icm* T4SS (55). Flagellin is recognized by the intracellular innate immune response proteins Naip5 and Nlrc4, members of the nucleotide-binding oligomerization domain (NOD) leucine-rich repeat (LRR) family of intracellular sensors (55, 56). Upon sensing flagellin, Naip5 binds Nlrc4, which recruits pro-caspase-1 into the newly assembled inflammasome (57). Once active, caspase-1 cleaves pro-interleukin 1β and interleukin 18 and also initiates pore formation in the macrophage cell membrane, leading to osmotic lysis and release of IL-1β and IL-18 (54, 58). In this way, the lysed macrophage releases pro-inflammatory cytokines and inhibits further replication of *L. pneumophila* (Figure 1.1).

Figure 1.1. *L. pneumophila in vivo* infection models in two genetically distinct mice.

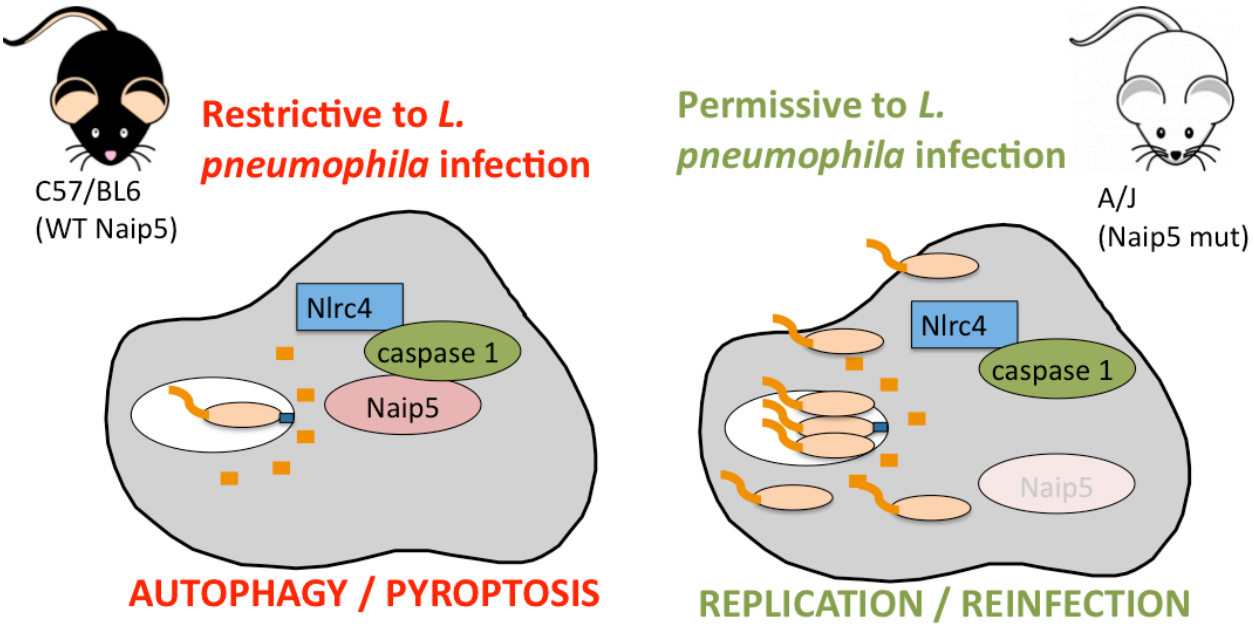

Bone marrow derived macrophages from C57/BL6 mice (left) are restrictive to *L. pneumophila* infection as they contain a WT copy of the NOD-like receptor NAIP5. Naip5 recognizes bacterial flagellin (orange squares) that leaks through the *dot/icm* T4SS during infection and subsequently recruits components of the Nlrc4 inflammasome complex. Production of pro-inflammatory cytokines leads to pyroptotic cell death and restriction of *L. pneumophila* infection. A/J derived macrophages carry a mutated copy of NAIP5 that is unable to recognize flagellin and activate the inflammasome. *L. pneumophila* is therefore able to replicate and is cytotoxic, allowing for escape and infection of a new host cell.

Components that govern the pyroptosis host defense pathway can be deduced by studying *L. pneumophila* infection in bone marrow-derived macrophages from mice of two distinct genetic backgrounds. C57/BL6 mice contain a wild-type copy of NAIP5 and are restrictive for infection, as the cytosolic immune surveillance system functions to clear *L. pneumophila* via pyroptosis or autophagy. A/J mice, however, carry a mutated copy of NAIP5; accordingly, these cells do not mount a robust inflammatory response to *L. pneumophila* exposure and allow bacterial replication and reinfection of new host macrophages (Figure 1.1). Thus C57/BL6 mice are restrictive to infection, and A/J mice are permissive.

L. pneumophila Genetic Diversity

Co-evolution of *Legionella* with phagocytic amoebae has led to horizontal gene transfer of several eukaryotic genes to *Legionella spp.*, a process thought to facilitate its adaptation to an intracellular lifestyle (59). Indeed, 55 proteins with eukaryotic domains have been identified in *L. pneumophila* strain Philadelphia. Several of these proteins are known *dot/icm* effectors and can modulate host cell functions (59). These effectors enhance virulence in human cells by disrupting host cell pathways to evade rapid delivery to degradative lysosomes, suppress activation of NF-kB and prevent host cell apoptosis (60). Similarly, acquisition of the amoebal glucoamylase GamA provides *Legionella* glycogen-degrading activity during intracellular replication in amoebae (61). Thus, ancestral acquisition of at least some of these eukaryotic proteins have

contributed to the evolution of diverse *Legionella* strains capable of infecting diverse types of phagocytes.

In general, *Legionella* exhibits a high degree of genome plasticity. Indeed, a survey of the genomes of six sequenced *L. pneumophila* strains determined that only ~80% of the genes are conserved and considered to be part of the core chromosome (62). The remaining ~20% of genes comprise the accessory genome, or gene components not necessary for bacterial replication. These genes are predicted to provide fitness advantages to or expand the host range of *L. pneumophila* in diverse environments or phagocytic hosts. Horizontal gene transfer of mobile elements between bacterial species can also drive the expansion of the accessory genome (59, 62). Among these strains, several accessory P, F and GI type T4SSs are present that appear to function independently of the *dot/icm* effector-secreting system (62, 63). Early studies confirmed that *L. pneumophila* carrying accessory plasmids persisted longer in the environment than those lacking plasmids (64). Indeed, upon closer examination, many of these accessory plasmids resemble ICEs and likely drive evolution of specific *L. pneumophila* subspecies.

ICEs in *L. pneumophila*

A comparative genomic survey of 217 serogroup 1 *L. pneumophila* clinical and environmental isolates revealed three highly variable regions among Philadelphia-1 strains (65). These plasticity zones all contain accessory T4SS and cargo components that resemble ICEs. Indeed, their heterogeneous distribution among this strain set

indicates the elements are mobilizable via horizontal gene transfer (65). Since initial identification, the 45-kb ICE-*lvh* T4SS region has been characterized as an ICE that can substitute for missing components in the *dot/icm* system and provides protection against water stress (66). A second 100-kb variable region (ICE-ice) contains a T4SS and a number of cargo genes predicted to be involved in resistance to metal ions (65, 67). The final region of plasticity identified in this study comprises a 65-kb region carrying a T4SS, integrase enzymes and a number of putative virulence factors (65, 68). This element is of particular interest as it is carried by 18% of isolates sampled and strongly resembles an ICE.

Outline of the Thesis

This thesis is built on the central hypothesis that *L. pneumophila* uses a diverse accessory genome to adapt to varied environmental conditions and niches. Its genomic diversity is expanded by the acquisition of self-transmissible mobile genetic elements such as ICEs. Despite the many species of *Legionella*, *L. pneumophila* causes 90% of Legionnaire's disease cases. The identification of a putative 65-kb ICE conserved in 18% of isolates screened suggests this ICE offers pathogenic strains fitness benefits and warrants further study. In Chapter Two, I dissect the contribution to *L. pneumophila* fitness of the 65-kb region, named ICE-βox. Confirmation of ICE-βox excision, transfer and integration into a new host confirms its designation as an ICE. Using a strain set containing or lacking the element, I show that ICE-βox confers to *L. pneumophila* strains the ability to resist *in vitro* and *in vivo* oxidative stresses in a manner dependent upon

the macrophage phagocyte oxidase. In Chapter Three, ICE-βox regulation is probed by detailed examination of the effects of a CsrA-like gene carried on the ICE. In Chapter Four, preliminary results of an epidemiological multiplex PCR screen for ICE-βox in *Legionella* isolates from the Center for Disease Control's strain collection are presented, and the findings of this thesis and their implications on *L. pneumophila* pathogenesis are discussed.

CHAPTER TWO

INTEGRATIVE CONJUGATIVE ELEMENT ICE-βOX CONFERS OXIDATIVE STRESS RESISTANCE TO *LEGIONELLA PNEUMOPHILA IN VITRO* AND IN MACROPHAGES

KJ Flynn and MS Swanson, *mBio* 2014 5(3):e01091-14

Summary

Integrative Conjugative Elements (ICEs) are mobile blocks of DNA that can contribute to bacterial evolution by self-directed transmission of advantageous traits. Here we analyze the activity of a putative 65-kilobase ICE harbored by *Legionella pneumophila* using molecular genetics, conjugation assays, a phenotype microarray screen and macrophage infections. The element transferred to a naive *L. pneumophila* strain, integrated site-specifically and conferred increased resistance to oxacillin, penicillin, hydrogen peroxide and bleach. Furthermore, the element increased survival of *L. pneumophila* within restrictive mouse macrophages. In particular, this ICE protects *L. pneumophila* from phagocyte oxidase activity, since mutation of the macrophage NADPH oxidase eliminated the fitness difference between strains that carried or lacked the mobile element. Re-named ICE-βox (for **β**-lactam antibiotics and **ox**idative stress),

this transposable element is predicted to contribute to the emergence of *L. pneumophila* strains that are more fit in natural and engineered water systems and in macrophages.

Introduction

Bacteriophage and transposable elements speed the spread of advantageous traits among bacterial populations, promoting genome diversity and evolution. The nosocomial lung pathogen *Legionella pneumophila* exhibits an extraordinary amount of genome plasticity, as up to 30% of six sequenced strain genomes is unique (62). Much of this variance is attributed to the acquisition of mobile elements (62), including Integrative Conjugative Elements (ICEs). ICEs are a class of transposons that encode type IV secretion systems (T4SS) that transfer by bacterial conjugation the core element as well as cargo genes that may confer fitness traits to the host (3). ICEs efficiently induce their own excision from the bacterial chromosome and subsequent site-specific integration into the chromosome of a new bacterium, ensuring the elements' propagation by the host replication machinery. By this mechanism, pathogens have acquired a variety of traits, including antibiotic resistance, biofilm formation, metal ion resistance and host invasion factors (3).

A number of ICEs have been identified in different strains of *L. pneumophila*. For example, *L. pneumophila* strain Corby encodes mobile ICEs (69, 70). Heterogeneity of the *L. pneumophila* genome was probed in a hybridization study of 217 clinical and environmental isolates (65). Three of the regions that are highly variable between isolates resemble ICEs that are predicted to enhance versatility. The *lvh* element of *L. pneumophila* strain Philadelphia-1, which is encoded by 67% of isolates examined,

restores entry and intracellular multiplication defects to mutants deficient in the canonical *dot/icm* T4SS (66). A second highly variable genomic region less frequent in this collection of *L. pneumophila* isolates (18%) is LpPI-1 (68). This 65-kb element (here re-named ICE-βox) is predicted to encode machinery for excision and transfer as well as a number of putative virulence factors and detoxifying enzymes (68).

To investigate the mobility and contribution of ICE-βox to *L. pneumophila* fitness, we applied genetic assays, a Biolog Phenotype MicroArray, *in vitro* growth analysis and macrophage infection studies on strains that contain or lack the element.

Experimental Procedures

Bacterial strains, culture conditions and reagents

L. pneumophila strain Philadelphia-1 derivatives JR32 and Lp02, a thymidine auxotroph, were cultured at 37°C in N- (2-acetamido)-2- aminoethanesulfonic acid (ACES; Sigma)-buffered yeast extract (AYE) broth supplemented with 100µg/ml thymidine (Sigma). To quantify colony forming units (CFU), aliquots were plated on ACES-buffered charcoal-yeast extract agar (CYE) supplemented with 100µg/ml thymidine (T) and incubated at 37°C for 4 days (71). Bacteria obtained from CYET were cultured overnight in AYET, then diluted and cultured overnight to obtain cells in lag (L; OD_{600} = 0.5), exponential (E; OD_{600} = 1.2-1.8), late exponential (LE; OD_{600} = 2.5) or post-exponential phase (PE; OD_{600} = 3.2-3.5) (53). *E. coli* strains DH5α and DY330 were cultured under standard laboratory conditions at 37°C and 30°C, respectively.

Penicillin G, oxacillin, gentamicin, chloramphenicol, and hydrogen peroxide were all purchased from Sigma. Bleach (Austin A-1, 6.15% NaOCl, 5.25% free chlorine) was purchased from Fisher Scientific. For bleach experiments, a new bottle was opened and diluted first in water, then AYET for use in growth experiments. Chlorine content in AYET broth was quantified using chlorine test strips (HACH) and estimated to be at a final concentration of 0.5ppm.

Mice

Six- to eight-week-old female A/J and C57BL/6 mice were purchased from Jackson Laboratories. Mice were housed in the University Laboratory Animal Medicine Facility at the University of Michigan Medical School under specific-pathogen-free conditions. The University Committee on Use and Care of Animals approved all experiments conducted in this study.

Generation of marked ICE-βox strains

The marked ICE-βox strain was generated by recombineering. The non-coding region between *lpg2110-2111* was amplified by PCR using primers 5'-GATAGCAGCATGTTTACTAGTCGG -3' and 5'- CGCATAACAAAGCGGCGC-3' and cloned into pGEM-T easy (Promega). After electroporation into *E. coli* strain DY330, λ-red recombinase replaced the corresponding ICE-βox non-coding region with a

chloramphenicol (cam) resistance cassette as described (72). The recombinant alleles were transferred to strain Lp02 via natural transformation to generate strain MB1353. Insertion of the cam cassette was confirmed by selection on CYET-cam and by PCR. Markerless deletions were created by electroporating pBSFlp into marked strains and selecting for the activity of the Flp recombinase to generate MB1357 and MB1358. Clones were screened for loss of the cam cassette by PCR and loss of pBSFlp by plating on selective medium.

Conjugation

To analyze ICE-βox transfer by conjugation, first the marked Lp02 donor strain MB1353 or the Lp02 control plasmid strain MB1326 were cultured to either E or PE phase, and the JR32 recipient strain MB1354 was cultured to PE phase. Next, 10^9 donor cells were mixed with 10^{10} recipient cells on 0.22µm filters placed on pre-warmed CYET agar plates with or without DNase I (1 µg/ml) and incubated for 2 h at 37°C as described (73). The mating mixture was harvested by suspending the filters in PBS and vortexing. Serial dilutions plated on CYET-cam (5 µg/ml) to select for donors or CYE-cam to select for transconjugants. Conjugation efficiency was calculated as CFU transconjugants / CFU donor cells. To test the impact of particular stresses on conjugation efficiency, donor cells were pre-treated in AYET for 1-2 h at 37°C with sublethal concentrations of penicillin G (5-10 µg/mL), oxacillin (50-100 µg/mL) or H_2O_2 (1-2mM).

Excision

Episomal ICE-βox was detected by a PCR assay using template DNA isolated from *L. pneumophila* colonies and specific primers (Table 2.1) to amplify either the chromosomal junction of ICE-βox or the junction of the episomal form as described previously (74). PCR products were column-purified (QIAquick, Qiagen) and sequenced using an Applied Biosystems Model 3730 XL sequencer. Integrated and excised forms of ICE-βox were quantified by qPCR using specific primers (Table 2.1) and 25 µg/mL template DNA prepared from strain Philadelphia-1 (Wizard SV Genomic kit, Promega), either cultured to different growth stages or treated with penicillin, oxacillin or H_2O_2 as described above. Reactions were carried out using a BioRad iCycler and SYBR Green (BioRad) according to the manufacturer's protocol. As an internal reference, the *rpoS* gene was used to normalize input DNA. Log_2 transformed values of the mean +/- SEM fold-change of episomal / chromosomal amplicons were calculated from three experiments performed in triplicate.

Phenotype microarrays and growth curves

A phenotype microarray screen was performed using PMA plates PM1 and PM12 from BIOLOG. Marked E phase ICE-βox donor MB1353, transconjugant MB1352 or MB1355 and recipient JR32 MB1354 cultures were diluted in AYET to OD_{600} of 0.2 and then 150 µl transferred per well of each BIOLOG plate. Plates were incubated at 37°C with shaking, and the OD_{600} was determined every 3 h using a plate spectrophotometer. Results of the BIOLOG screen were verified by growth curve assays. Strains were

cultured in AYET to E phase, diluted and cell density normalized to OD_{600} 0.2 for triplicate samples. Bleach was diluted in water and added to the cell suspension to a final concentration of 55 ppm. Growth was quantified hourly by OD_{600} using a Bioscreen Growth Curve Analyzer set at 37°C and shaking at medium amplitude. Stress resistance was assessed by quantifying CFU after treating triplicate E phase samples sub-cultured in AYET to OD_{600} of 0.8 for 6 h with penicillin, oxacillin and H_2O_2 as described. Mean +/- SEM fold change was calculated as CFU at 6 h / CFU at 0 h from three independent experiments. As an additional specificity control, recipient strains transformed with plasmid-born cam resistance cassette (MB1351) were analyzed in each experiment that used marked strains.

Intracellular growth and immunofluorescence microscopy

Growth of *L. pneumophila* strains containing or lacking ICE-βox (Donor MB1353, Transconjugant MB1352 and Recipient MB1351) was assessed in bone marrow-derived macrophages from C57BL/6 or A/J mice (Jackson Laboratories) as described (75). Means +/- SD were calculated from triplicate samples. Microscopy was performed by culturing 2.5 x 10^5 macrophages on 12mm glass coverslips overnight prior to infection with PE phase bacteria at an MOI of 1. After 24 h, cultures were fixed and stained as described (47) using a 1:50 dilution of anti-*L. pneumophila* primary antibody obtained from mouse monoclonal hybridoma cell line CRL-1765 (ATCC) and a 1:1000 dilution of anti-mouse IgG antibody conjugated to Oregon Green (Molecular Probes). The DNA

Table 2.1: Primers used in Chapter Two

Primer name	**Primer (5' to 3')**
P1 fwd	GATGGGTATAGGAGAGCGTGGTTG
P2 rev	CCGCTCGAAATGCCACCTC
P3 fwd	GGCATGACTTGCGTCACACTTG
P4 rev	GCTCAGGTGGTAGAGCAGGAGG
qPCR P1 fwd	AATTTGAGAGTGGTTGCGCTAT
qPCR P2 rev	TGGCTTCGAACCAAGGTGT
qPCR P3 fwd	CTTGGTTTTTACGGCACGTT
qPCR P4 rev	ACCATTCTGGTCTCCCTCCT
rpoS qPCR fwd	CTCCAAAGGCTTATCCACCA
rpoS qPCR rev	TGAGAAATTTGACCCCAAGC

stain DAPI (4',6-diamidino-2-phenylindole) was purchased as ProLong Gold Anti-Fade reagent (Molecular Probes) and included in the mounting medium. NADPH oxidase experiments were performed using a pair of cell lines derived from BALB/c mouse background. J774.16 (WT) and J774.D9 phox (deficient in gp91 subunit of NADPH oxidase) cells were infected as above (76).

Results

L. pneumophila ICE-βox excision, transfer and site-specific integration

ICEs promote their own conjugative transfer by encoding a type IV secretion system and integrase. To determine whether ICE-βox can spread to a naïve bacterial recipient, we performed conjugation assays using a donor that carried a genetically marked ICE-βox. For this experiment, we exploited known differences in two derivatives of the *L. pneumophila* strain Philadelphia-1. Strain Lp02 encodes ICE-βox, but JR32 does not (77); therefore, ICE-βox-marked Lp02 cells served as the donor and naïve JR32 as the recipients. Indeed, like a control plasmid that encodes an *oriT* sequence, ICE-βox transferred from donor to recipient cells by a process insensitive to exogenous DNase I (Figure 2.1B). ICE-βox transfer was ~10-fold more efficient when donor cells were in exponential phase ($P < 0.01$) versus post-exponential phase.

To determine whether ICE-βox integrated into the chromosome of the transconjugant strain, we applied a PCR assay (74). Specific primer sets (Figure 2.1C)

Figure 2.1. ICE-βox is a mobile genetic element

A) Schematic of ICE-βox. The 65-kb locus is predicted to encode 38 cargo (spotted), 4 regulatory (gray) and 18 type IV secretion system (T4SS, striped) genes. ICE-βox is flanked by 43-bp direct nucleotide repeat regions deduced to serve as attachment sites (*attL* and *attR*). The drawing is not to scale.

B) ICE-βox transfer by exponential and post-exponential phase cells is resistant to DNase I. Plating on selective medium identified control plasmid or ICE-βox transconjugants. The mean efficiency +/- SEM was calculated from three experiments as # ICE-βox-positive JR32 recipient cells / donor cell. More efficient conjugation by E than by PE phase cells was statistically significant according to the student's T test (**, $P < 0.01$).

C) Schematic of ICE-βox excision assay. Specific primer sets P1/P2 and P3/P4 amplify the *attL* and *attR* junction fragments, respectively, whereas P2/P3 generate a product (*attI*) from excised ICE-βox, and P1/P4 amplify the attachment site remaining in the chromosome after excision (*att*).

D) PCR detects circularized ICE-βox. Using the PCR assay described in (A) and genomic DNA isolated from *L. pneumophila* Donor (Lp02, MB1353), Recipient (JR32, MB1354) and Transconjugant (JR32+ ICE-βox, MB1354), junction fragments for integrated (*attL, attR*) and excised ICE (*attI*) forms of ICE-βox were detected as well as the site remaining after excision (*att*).

Figure 2.1. ICE-βox is a mobile genetic element

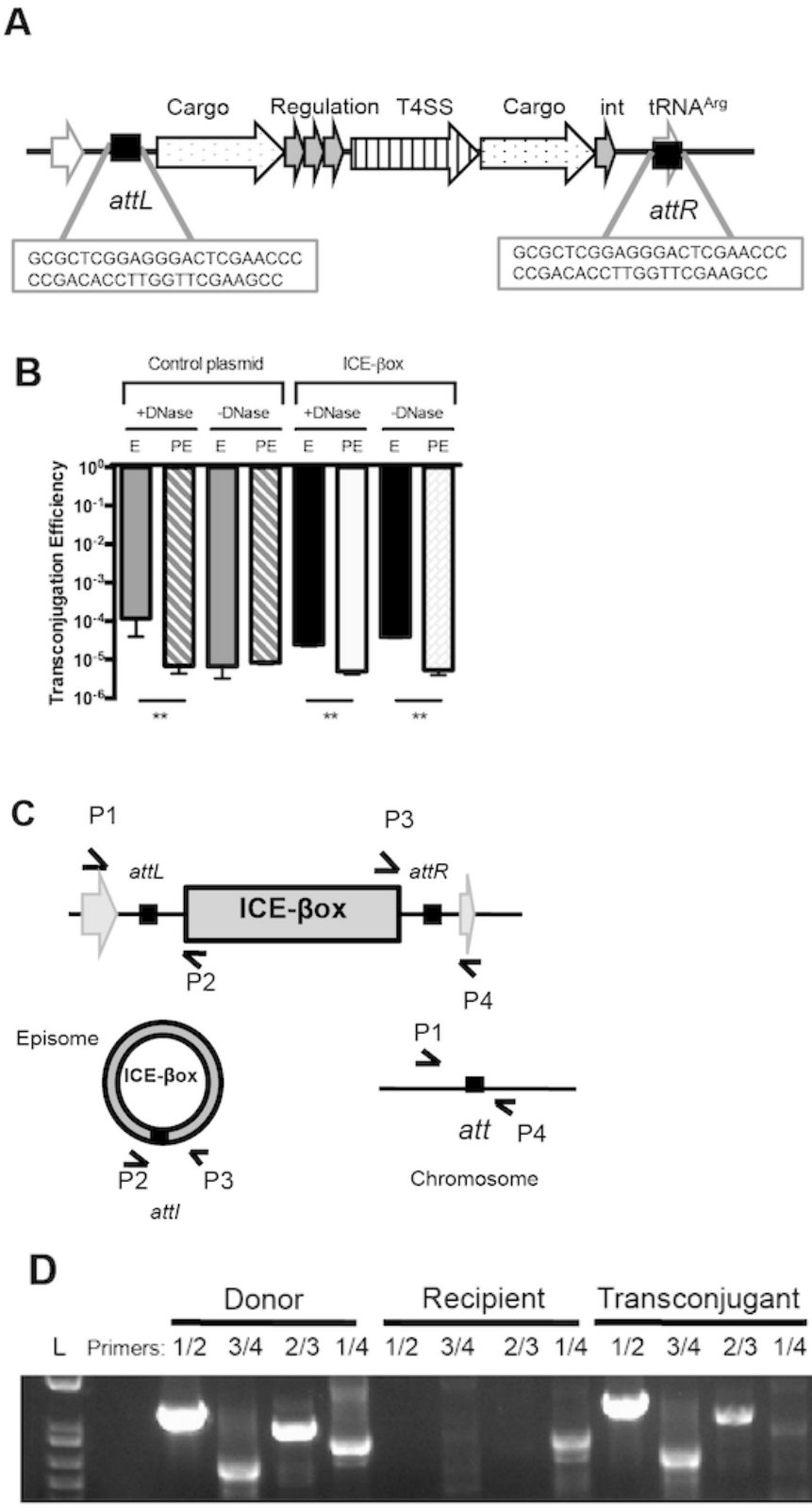

P1/P2 or P3/P4 amplify 5' or 3' junction fragments of ICE-βox that is integrated into the chromosome (*attL* and *attR,* respectively), whereas primers P2/P3 generate a product from elements that are excised and circularized (*attI*) and P1/P4 amplify the scar site after excision (*att*). Although no integrated or excised ICE-βox product was generated from recipient JR32 DNA, both integrated and episomal forms of ICE-βox were detected within a population of cells of the *L. pneumophila* Lp02 donor and the transconjugant strain, and all strains harbored the *att* site necessary for re-integration of ICE-βox into the chromosome (Figure 2.1D). In multiple independent experiments we consistently observed less *attI* and *att* product in the transconjugant population. Perhaps variability in band intensity for the *attI* and *att* forms of ICE-βox in the transconjugant reflects differential regulation of excision in this strain background.

ICEs integrate into bacterial chromosomes by homologous recombination of direct nucleotide repeat sequences (3). To confirm the integration site of the element, the DNA sequence of the chromosomal and episomal amplicons (*attL, attR, attI*) generated as described in Figure 2.1D was determined. An identical 43-bp sequence flanked each side of ICE-βox and the excised form (Figure 2.1A). One copy of the repeat sequence was located within a chromosomal $tRNA^{Arg}$ gene, consistent with other known ICEs and the genomic sequences of the Philadelphia-1, Lp02 and JR32 strains (77, 78).

Since the *lvh* ICE excises more efficiently in post-exponential phase cells (Figure 2.2A) (74), we measured the impact of growth phase on ICE-βox excision. Unlike *lvh*, ICE-βox excision is not sensitive to growth phase in rich medium. Analysis by qPCR of template

DNA isolated from cultures at different growth phases determined an excision ratio of ~3 – 5 x 10^{-8} episomes per chromosome at each time point (Figure 2.2B). Since ICE-βox excises, mobilizes and integrates site-specifically into a new host chromosome, its designation as an ICE is confirmed.

ICE-βox confers resistance to β-lactam antibiotics, hydrogen peroxide, and bleach *in vitro*

As a strategy to identify traits conferred by ICE-βox, we used BIOLOG Phenotype MicroArrays to compare the growth of donor and ICE-βox transconjugant strains to that of naïve recipient cells. All strains replicated with equal efficiencies in standard growth medium. Of the 200 different carbon sources and growth inhibitors tested, the most striking differences were observed for two β-lactam antibiotics, oxacillin and penicillin. Subsequent growth curve experiments confirmed that the ICE-βox-containing donor and transconjugant *L. pneumophila* strains tolerated these antibiotics, but the naive recipient strain did not (Figure 2.3A, 2.3B). We verified that ICE-βox promotes bacterial survival and replication by quantifying CFU after a 6 h exposure to 100 μg/mL oxacillin or 2 μg/mL penicillin G (Figure 2.3C).

β-lactam antibiotics are known to induce production of reactive oxygen species (ROS) as an indirect consequence of crosslinking cell-wall peptidoglycan (79). Therefore, to test whether ICE-βox confers protection from ROS, we quantified resistance to hydrogen peroxide. Similar to the β-lactam antibiotics, ICE-βox enhanced resistance to this oxidative stress (Figure 2.3C). We next tested the ability of ICE-βox to

Figure 2.2 ICE-βox excision is not coordinated with growth phase

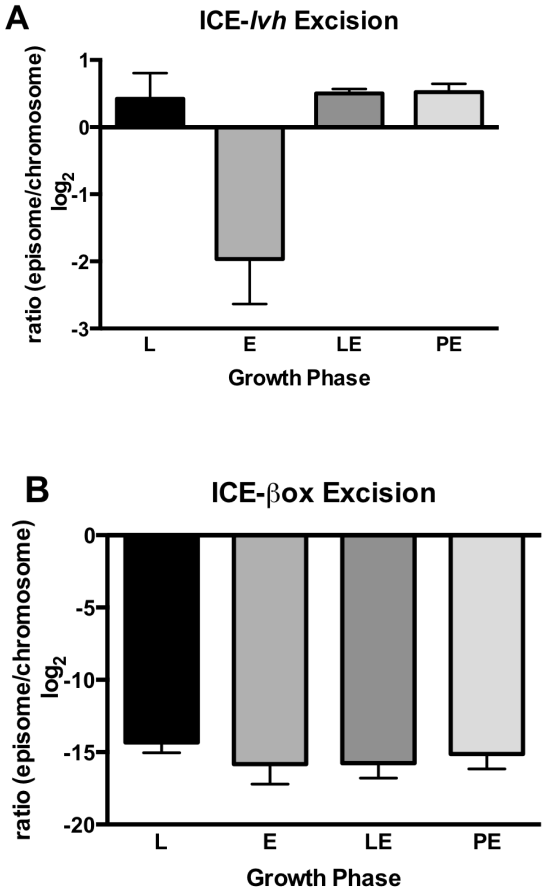

A, B) qPCR analysis indicates ICE-βox excision is not coordinated with growth phase. To determine excision frequency, the assay described in (Figure 2.1A) was performed quantitatively using DNA isolated from *L. pneumophila* Philadelphia-1 strains cultured to lag (L), exponential (E), late exponential (LE) or post-exponential (PE) phases. Excision was determined using primer sets specific for ICE-*lvh* (A) or ICE-βox (B). The abundance of excised ICE was compared to integrated ICE using the ΔΔCT method, normalizing to chromosomal gene *rpoS*. Shown are means +/- SEM of three independent experiments.

Figure 2.3. ICE-βox promotes oxidative stress survival.

A, B) ICE-βox confers resistance to oxacillin and penicillin. E phase cultures of ICE-βox Donor (D, circles), Recipient (R, squares) or Transconjugant (T, triangles) were exposed to 100μg/mL oxacillin (A) or 2μg/mL penicillin G (B), and at the times shown their growth quantified as optical density at 600nm by a Bioscreen growth curve analyzer. Shown are means +/- SEM calculated from triplicate samples in one experiment representative of three others. T-tests indicate differences between strains that encode or lack ICE-βox are statistically significant (****, $P < 0.001$).

C) ICE-βox increases *L. pneumophila* resistance to oxacillin, penicillin and hydrogen peroxide. E phase cultures of ICE-βox Donor (D, black), Recipient (R, white) or Transconjugant (T, gray) strains that contained or lacked ICE-βox were exposed for 6 h to 100μg/mL oxacillin, 2μg/mL penicillin G or 2mM H_2O_2, and then mean survival +/- SEM was calculated from three independent experiments as (CFU treated) / (CFU untreated). T-tests indicate differences between strains that encode or lack ICE-βox are statistically significant (***, $P < 0.005$).

D) ICE-βox increases *L. pneumophila* resistance to bleach. E phase cells of ICE-βox Donor (D, circles), Recipient (R, squares) or Transconjugant (T, triangles) strains were cultured with 0.5ppm bleach and optical density at 600nm recorded at the times shown using a Bioscreen growth curve analyzer. Shown are means +/- SEM calculated from three replicates in one experiment representative of three others. Multiple t-tests indicate differences between strains that encode or lack ICE-βox are statistically significant (**, $P < 0.01$)

Figure 2.3. ICE-βox promotes oxidative stress survival.

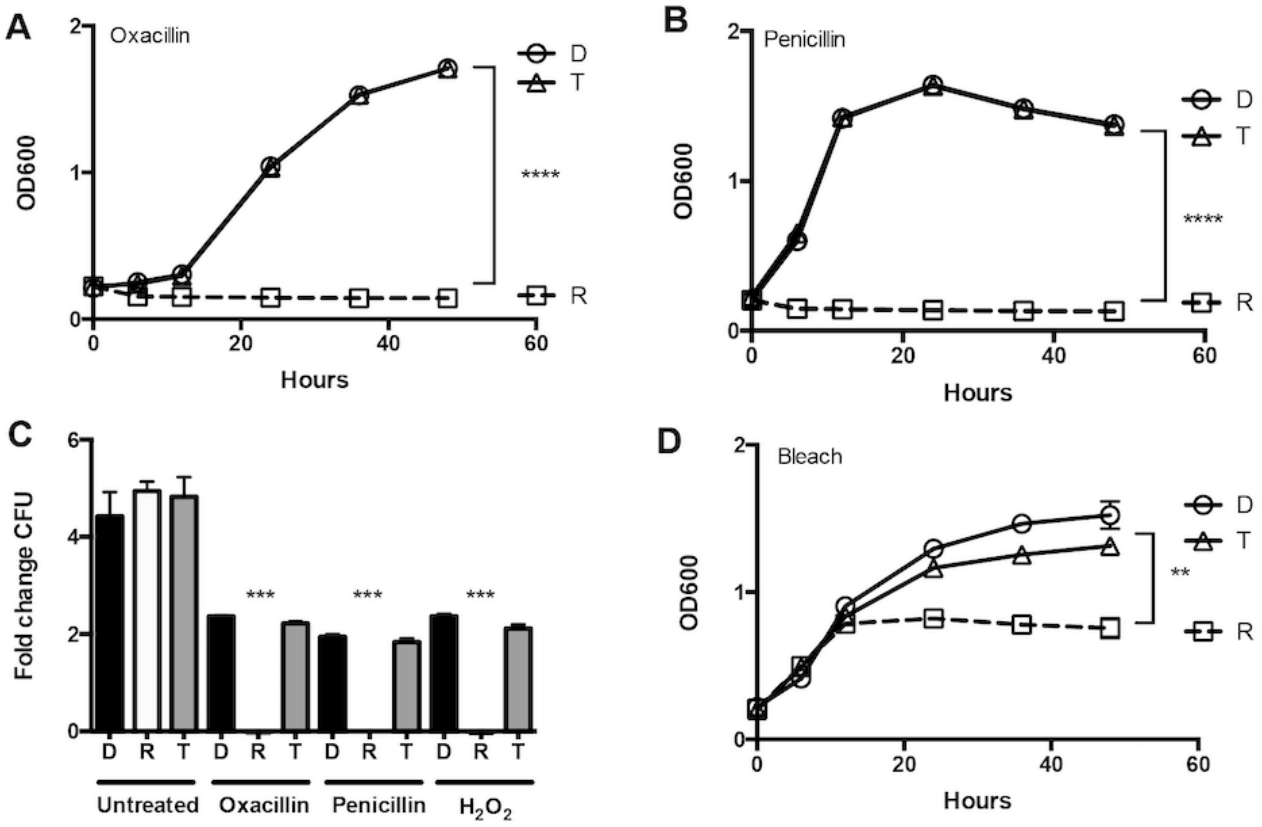

protect *L. pneumophila* from bleach (NaOCl) a common disinfectant that contains both reactive oxygen and chlorine. As observed for the other oxidative stresses tested, donor and transconjugant strains that carried ICE-βox survived and replicated in culture medium supplemented with bleach to 0.5ppm, a concentration typical of drinking water (Figure 2.3D) (80). For all phenotypic tests, three additional independent transconjugant strains and two markerless ICE-βox derivatives exhibited a similar pattern of resistance (data not shown). Thus, ICE-βox increases *L. pneumophila* fitness by protecting cells from β-lactam antibiotics, hydrogen peroxide and bleach, three sources of oxidative stress.

External oxidative stress does not induce ICE-βox excision and transfer

For some elements, ICE excision and transfer is controlled by regulators encoded on the island that respond to the same stressful stimuli from which the ICE protects (16). Since ICE-βox conferred resistance to agents known to inflict oxidative stress (Figure 2.3), we investigated whether these treatments induce ICE-βox mobility or transfer. *L. pneumophila* ICE-βox donor cells were exposed for 1 h to oxacillin, penicillin or hydrogen peroxide and then assayed for excision and transfer. ICE-βox excision was not significantly induced after the 1 h exposure to these oxidants, as judged by qPCR assays on isolated DNA (Figure 2.4A). Even across a range of chemical concentrations and mating periods, transfer rates of ICE-βox from treated cells did not differ significantly from control levels (Figure 2.4B). Accordingly, these oxidative stresses do not appear to stimulate ICE-βox mobility.

Figure 2.4. Oxidative stress has minimal effect on ICE-βox mobility

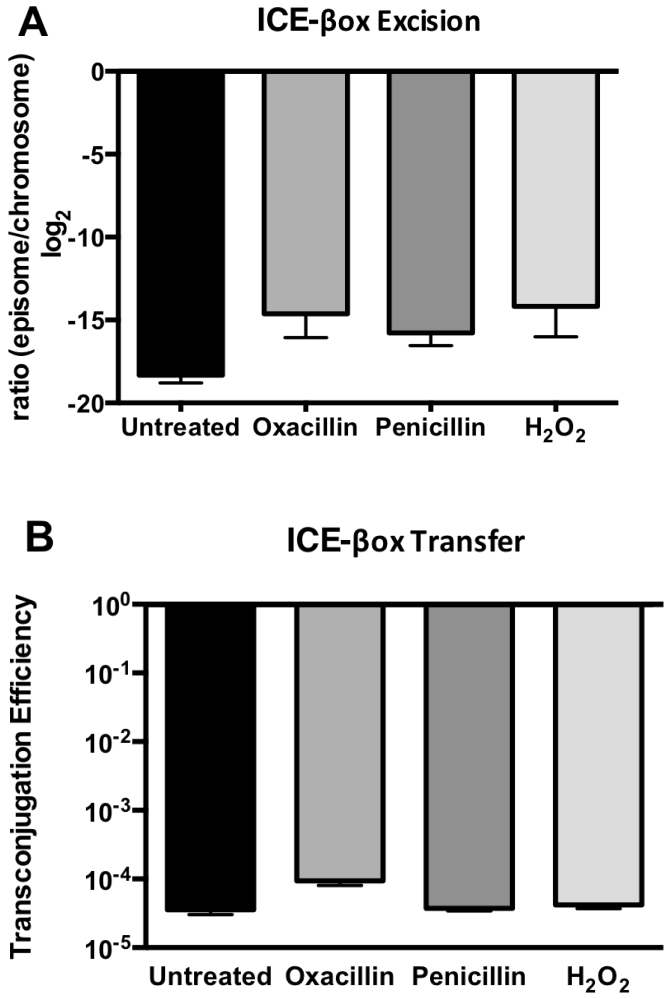

A) ICE-βox excision. qPCR excision was quantified as described using template DNA prepared from cultures exposed for 1 hr to 100μg/mL oxacillin, 2μg/mL penicillin G or 2mM H_2O_2. Shown are means +/- SEM calculated from three independent isolates in one experiment representative of 4 others.

B) ICE-βox transfer. Conjugation was quantified after treatment for 1 hr with or without oxidative stresses as described above. Shown are means +/- SEM calcuated from three replicates in one experiment representative of 4 others.

Figure 2.5. ICE-βox confers protection to *Legionella* in resistant macrophages.

A) ICE-βox increases fitness in permissive A/J macrophages. Macrophages were infected at an MOI of 1 with *L. pneumophila* that contain or lack ICE-βox. Shown are mean CFU +/- SEM calculated at the times shown from triplicate samples in one experiment representative of three others. T-tests indicate growth differences between ICE-βox containing and lacking strains are significant (****, $P < 0.001$).

B) ICE-βox increases *L. pneumophila* persistence in activated A/J macrophages. Macrophages were activated with 100U IFN-g were infected at an MOI of 1 with *L. pneumophila* that contain or lack ICE-βox. Shown is the mean +/- SEM fold change in CFU at the times shown post infection relative to the 2 h time point calculated from triplicate samples in one experiment representative of three others. T-tests indicate differences between ICE-βox containing and lacking strains are significant (***, $P < 0.005$).

C) ICE-βox increases *L. pneumophila* persistence in resistant BL/6 macrophages. After infecting BMM as described in (A), mean CFU+/- SEM was calculated from three replicates in one experiment representative of three others. T-tests indicate differences between ICE-βox containing and lacking strains are significant (***, $P < 0.005$).

D, E) ICE-βox protects *L. pneumophila* from degradation in B6 macrophages. 24 h after infection bacterial integrity was visualized by immunofluorescence microscopy using *L. pneumophila*-specific antibody (green) and the DNA stain DAPI (blue). Shown are the mean % +/- SEM of macrophages that contained degraded bacteria calculated from three replicates in one experiment representative of three others. (E) Representative images of infected B6 macrophages shown. T-tests indicate differences between ICE-βox containing and lacking strains are significant (**, $P < 0.01$).

F, G) ICE-βox's protective effects are dependent on NADPH-oxidase. WT (F) or NADPH-oxidase mutant (G) J774 cell lines were infected at an MOI of 1 with *L. pneumophila* containing or lacking ICE-βox. Shown are mean CFU +/- SEM calculated from three replicates in one experiment representative of three others. T-tests indicate differences between ICE-βox containing and lacking strains are significant in WT macrophages (**, $P < 0.01$).

Figure 2.5. ICE-βox confers protection to *Legionella* in resistant macrophages.

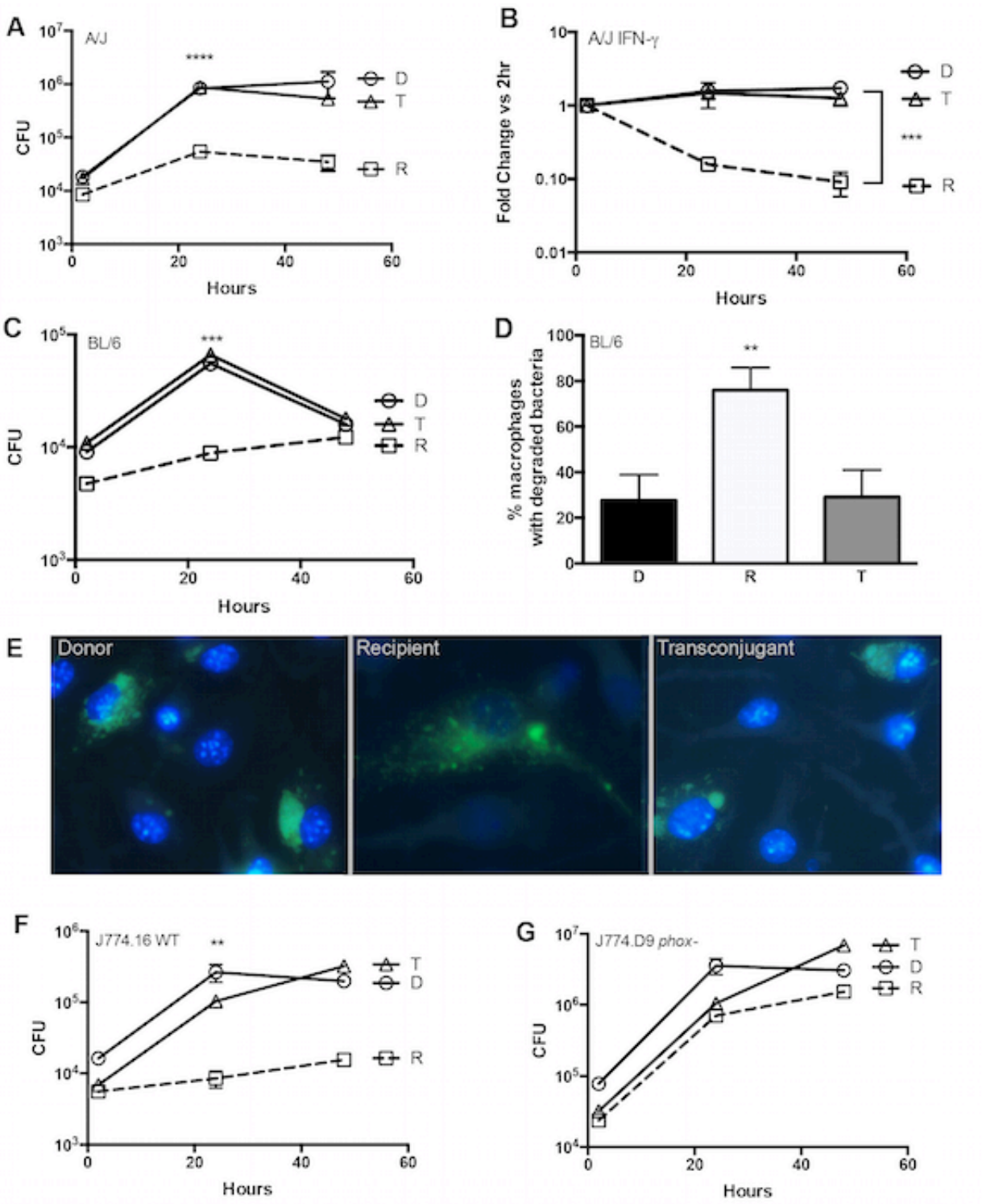

ICE-βox confers protection to *L. pneumophila* in stringent macrophages

In human lungs, macrophages are the opportunistic host for *L. pneumophila*. Since ICE-βox increased resistance to oxidative stress *in vitro*, we next tested whether ICE-βox enhances protection in macrophages, immune cells that generate reactive oxygen species to kill microbes (81). A/J mice are permissive to *L. pneumophila* infection due to mutations in their Naip5 cytosolic surveillance protein (82). After 48 h in primary macrophages derived from A/J bone marrow cells, the yield of ICE-βox donor and transconjugant bacteria increased ~100-fold, whereas the recipient strain was significantly impaired (Figure 2.5A). As a more stringent test of the impact of ICE-βox on *L. pneumophila* virulence, we next stimulated permissive A/J macrophages with IFN-γ. Activated A/J macrophages killed the recipient strain that lacked ICE-βox, whereas the donor and transconjugant strains that harbored the ICE survived (Figure 2.5B). We next tested whether ICE-βox increased *L. pneumophila* fitness in macrophages of Naip5$^{+/+}$ C57BL/6 mice, which are resistant to *L. pneumophila* infection (82, 83). During the first 24 h of infection of C57BL/6 bone marrow-derived macrophages, strains that encode ICE-βox replicated within macrophages ~ 10-fold more efficiently than those that lacked the element ($P < 0.005$) (Figure 2.5C). The fate of the intracellular bacteria was confirmed by examining the infected macrophages by fluorescence microscopy. At 24 h after infection, recipient bacteria that lack ICE-βox were degraded, as evident from the particulate *L. pneumophila* antigen scattered throughout the cell (Figure 2.5D, E). In contrast, multiple ICE-βox-containing donor and transconjugant bacteria resided within tight replication vacuoles (Figure 2.5E), consistent with their increased yield (Figure

2.5C). Therefore, ICE-βox enhances *L. pneumophila* infection and persistence within hostile mouse macrophages.

ICE-βox protection in macrophages is NADPH oxidase-dependent

To test directly whether ICE-βox increases resistance to phagocyte oxidases, we compared *L. pneumophila* growth in macrophages that encode or lack a component of the NADPH oxidase. For this purpose, we exploited a pair of BALB/c mouse derivative J774 WT and *phox* mutant macrophage cell lines (76). Infection of WT J774.16 cells by *L. pneumophila* strains that do or do not carry ICE-βox revealed a pattern similar to that observed for the infections of A/J and C57BL/6 primary macrophages. The yield of *L. pneumophila* that encode ICE-βox increased ~10-fold within the first 24 h, compared to < 2-fold increase in CFU for bacteria that lack the element (Figure 2.5F). In contrast, after infection of J774.D9 *phox* mutant cells, all strains replicated > 50-fold, regardless of their ICE-βox status (Figure 2.5G). Therefore, ICE-βox increases *L. pneumophila* fitness within macrophages that encode NADPH oxidase.

Discussion

ICEs contribute virulence and fitness traits to a wide array of pathogens, including *Vibrio cholerae*, *Pseudomonas aeuriginosa* and *Staphylococcus aureus*. Here we describe a transposable element named ICE-βox to emphasize its capacity to protect *L. pneumophila* from **β**-lactam antibiotics and **ox**idative stresses. Because aerosolization of environmental *L. pneumophila* is a prerequisite for infection (84),

microbial factors that increase extracellular survival may also contribute to transmission to humans. Given the capacity of ICEs to transfer between nosocomial pathogens and to increase microbial fitness, the impact of water decontamination protocols on the incidence of human disease caused by *L. pneumophila* warrants analysis.

Although, strain Philadelphia-1 is the only one of the eight *L. pneumophila* strains sequenced to date that encodes ICE-βox, homology searches revealed all eight strains contain the 43-bp *att* site for integration. Thus, it is likely that ICE-βox can spread among *L. pneumophila* strains. Loss of the element during derivation of the JR32 strain from the Philadelphia-1 clinical isolate (77) is consistent with the idea that ICE-βox is readily mobilized in certain environmental conditions. Exploratory experiments with *E. coli, V. cholerae* and *P. aeuriginosa* indicate *L. pneumophila* can transfer ICE-βox to other pathogens, but the element is not stably maintained, as judged by loss of its antibiotic resistance marker during subsequent passage of the respective transconjugant strains (data not shown). These genetic observations suggest chromosomal maintenance of ICE-βox requires conserved *att* sites (Figure 2.1A), a sequence not detected by *in silico* analysis of *E. coli, V. cholerae* and *P. aeuriginosa* or other non-*L. pneumophila* species.

To activate transcription of their genes, ICEs often integrate the regulatory circuitry carried on the element with core bacterial response systems, such as the SOS response (3). The ICE-βox region is rich with putative regulators, including homologs of the global regulators *csrA* and *lexA*, a small non-coding RNA located adjacent to the *att* sites, and putative diversity-generating retroelements (DGR) that alter expression of

certain *L. pneumophila* traits (85). Indeed, the homologous region of ICE Trb-1 in *L. pneumophila* strain Corby has been shown by mutational analysis to regulate site-specific excision (70). Insight to the regulation of ICE-βox cargo gene expression can be gained by molecular genetic analysis of this class of genes.

Among the 38 predicted cargo genes carried by ICE-βox are a number of stress response enzymes (68). Near its 3' end is a putative oxidative stress resistance operon that encodes two copies of the detoxifying enzyme genes *m*ethionine *s*ulfoxide *r*eductase A and B (*msrAB)*, as well as a cytochrome C oxidase (*lpg2100*) and an alkyl hydroperoxide reductase (*ahp*) homolog. The *msrAB* locus is of particular interest since in *Staphylococcus aureus msrA* transcription is upregulated in response to oxacillin (86). Additionally, *msrA* protects *E. coli* from hydrogen peroxide-induced killing (87) and increases tolerance of the intracellular *Mycobacterium smegmatis* to macrophage NADPH oxidase (88). Likewise, *ahp* homologs equip *Salmonella* to scavenge free hydrogen peroxide and survive macrophage infection (89). Given their contribution to virulence in other pathogens, these enzymes are primary candidates to investigate the biochemical mechanism of protection by ICE-βox. Since the core chromosome of *L. pneumophila* also encodes *msrA* and *ahpCD* genes, we speculate that a higher level of expression from the additional copies on ICE-βox increases *L. pneumophila* resistance to oxidative stress.

L. pneumophila persists in water supplies likely due its ability to reside within both hardy biofilms and predatory amoebae (90). We did not detect any differences in the ability of ICE-βox-containing or -lacking strains to replicate within *Acanthamoeba*

castellanii (data not shown). Nevertheless, ICE-βox may contribute to increased survival in other aquatic phagocytes, as *L. pneumophila* is known to infect numerous amoebae species whose permissiveness varies (91, 92).

A remarkable finding is that samples from hospitals, schools and spas contained a higher density of *Legionellae* than their source water (93), suggesting that, relative to the natural environment, engineered water systems offer some advantage to this species. Typical hospital disinfectant regimens generate reactive chlorine species (RCS) oxidants from bleach, monochloramine or chlorine dioxide (94). However, infection control treatments reduce but do not eliminate the pathogen (93), implying that a subpopulation of *L. pneumophila* is resistant to or protected from these chemicals. Indeed, in a survey of 209 samples from Paris hospitals, use of continuous chlorination protocols correlated with an increase in the burden of pathogenic serogroup 1 *L. pneumophila* in their engineered water systems (44). Our findings show ICE-βox promotes survival and replication in bleach concentrations comparable to that typical of drinking water (80). Given widespread use of ROS and RCS in water decontamination procedures and the conservation of the *att* sites among *L. pneumophila* strains, the potential for spread of disinfectant resistance among populations of this opportunistic aquatic pathogen merits consideration.

Beyond increasing fitness in the environment, resistance to oxidative stress also enhances virulence. Production of ROS is a primary mechanism of the macrophage antibacterial response. Bacterial entry induces cellular NADPH oxidase to generate superoxide and hydrogen peroxide, which myeloperoxidase enzymes subsequently

convert to the reactive chloride species HOCl (95, 96). Here we have shown that *L. pneumophila* that acquire resistance to chlorine and oxidative stress also become more virulent in macrophages. Given this transposable element's ability to increase fitness of planktonic bacteria in a variety of oxidizing conditions both *in vitro* and in macrophages, we postulate that ICE-βox increases the burden and virulence of pathogenic *L. pneumophila* in natural and engineered environment.

CHAPTER THREE

CsrA PARALOG CsrT REGULATES CORE AND ACCESSORY GENOME TRAITS IN *LEGIONELLA PNEUMOPHILA*

ZD Abbott*, KJ Flynn*, BG Byrne, S Mukherjee, D Kearns, MS Swanson.
*denotes coauthorship. *Submitted.*

Statement of contribution: Z.D.A proposed the project and designed most experiments. Z.D.A, K.J.F., B.G.B. and S. M. performed the experiments and analyses. Z.D.A and K.J.F. wrote the paper.

Summary

Bacterial evolution is accelerated by mobile genetic elements. To spread horizontally and to benefit the recipient bacteria, genes encoded on these elements must be properly regulated. Among the legionellae are multiple Integrative Conjugative Elements (ICEs) that each encode a paralog of the broadly conserved regulator *csrA*. Using bioinformatic analyses, we deduced that specific *csrA* paralogs are co-inherited with particular lineages of the type IV secretion system that mediates horizontal spread of the ICE, suggesting a conserved regulatory interaction. To investigate the contribution of *csrA* to this class of mobile genetic elements, here we analyze the function of *csrT*, the *csrA* paralog encoded on *L. pneumophila* ICE-βox. CsrT abrogated the protection to hydrogen peroxide and macrophage degradation ICE-βox confers to *L. pneumophila*. In addition to modulating expression of some ICE-encoded cargo genes, CsrT also repressed *L. pneumophila* flagellin production and motility, a broadly

conserved core genome trait that contributes to *L. pneumophila* transmission in water and virulence. Likewise, *csrT* repressed motility of *B. subtilis csrA* mutants, consistent with its predicted function as an mRNA-binding protein. That all known ICEs of legionellae encode co-inherited *csrA* – type IV secretion system pairs suggests the capacity of CsrA superfamily proteins to regulate both ICE and host traits increases ICE promiscuity and expands *L. pneumophila* versatility.

Introduction

Mobile DNA elements can spread advantageous traits among bacterial populations and contribute to the evolution of pathogens (3). Integrative Conjugative Elements (ICEs) are one type of mobile transposable element that encode their own type IV secretion system (T4SS) for transfer between strains and also the enzymes necessary to integrate the element into the host chromosome. ICEs have expanded the genetic repertoire of a number of bacterial pathogens by carrying a variety of cargo genes that confer advantageous traits upon their host. Some confer resistance to antibiotics, metal ions and oxidative stress; others enhance nitrogen and chlorobenzoate metabolism, biofilm formation and host cell infection (16, 97-99). Separate from the cargo genes are those encoding the elements' structural components, which are also diverse. Distinct classes of T4SSs mediate ICE transmission within and between species (2). Such diversity may permit multiple ICEs to be maintained within one bacterial cell (100).

Bacteria coordinate expression of multiple extracellular structures, each with distinct purposes. *L. pneumophila* produces short pili for adherence or long T4SS conjugative pili for effector secretion or horizontal gene transfer, but not both pili at the same time (101). Likewise, simultaneous expression of similar T4SS by *L. pneumophila* is counter-productive, as activity of the core Dot/Icm T4SS is inhibited by the MobA component of a related RSF1010 conjugative plasmid (102). Accordingly, competition between ICEs likely provides selective pressure for regulatory circuits that ensure reciprocal expression of their T4SS machines.

The regulatory mechanisms governing the expression of ICE traits are as diverse as the ICEs themselves. For example, SXT from *Vibrio cholerae* and ICEBs1 from *Bacillus subtilis* encode regulatory genes that are cleaved or bound by host regulators induced by the bacterial SOS response (19, 103). Other ICEs are equipped with regulatory circuitries that act independently of host proteins. ICEclc from *Pseudomonas aeruginosa* and CTnDOT from *Bacteriodes thetaiotaomicron* carry sensor proteins that respond to chlorobenzoate or tetracycline, respectively; these chemicals induce transcription of regulatory genes that drive expression of cargo loci that confer protection from these stressors (104, 105). Other ICEs, such as pLS20 from *B. subtilis* and pAD1 of *Enterococcus faecalis*, rely on secreted peptides or pheromones, respectively, to sense recipient cells in the environment and then induce a signaling cascade that activates transcription of the conjugative pilus (106, 107). Finally, to regulate transfer, the *Agrobacterium tumefaciens* Ti conjugative plasmid responds to the secreted quorum sensing N-acyl-L-homoserine lactone (AHL) molecule (108).

The environmental and opportunistic pathogen *Legionella pneumophila* typically carries multiple ICEs in its genome. For instance, the Philadelphia-1 strain of *L. pneumophila* harbors three distinct ICEs (109). One of these mobile elements, ICE-βox, enhances the pathogen's resistance to bleach and the β-lactam antibiotics oxacillin and penicillin (97). Strains that carry ICE-βox are also more infectious and tolerant of the macrophage phagocyte oxidase (97). Protecting the bacterium from these stresses presumably benefits ICE-βox by ensuring a healthy host competent for spread of the element. Thus, expression of the ICE-βox-encoded T4SS transmission machinery and cargo traits must be regulated in a manner that ensures ICE-βox maintenance.

It is striking that ICE-βox encodes a paralog of *csrA,* a key regulator of *L. pneumophila* differentiation. The canonical CsrA is encoded in the "core" genome: it is ubquitous and highly conserved in the *Legionella* genus and is not encoded within a horizontally acquired genetic element (65, 67). CsrA is a broadly conserved mRNA binding protein that is essential for *L. pneumophila* replication and that represses numerous *L. pneumophila* transmissive phase traits, including expression of substrates of the core Dot/Icm T4SS (110, 111). Furthermore, similar to the dual CsrA system in *P. aeruginosa* (112), CsrA directly represses *csrR*, a newly identified *csrA* paralog in the *L. pneumophila* core genome, a design predicted to establish a reciprocal expression profile (Abbott 2015, in review). The legionellae also encode a large "accessory" genome: highly variable regions of the genome frequently composed of horizontally acquired elements, including ICEs, that are not conserved between strains and species (62, 63, 113). The ICE Trb-1 mobile element in the accessory genome of *L.*

pneumophila strain Corby also encodes a *csrA* paralog, *lvrC* (70). The *lvrC* locus encodes a repressor of ICE Trb-1 mobility, as deletion of the four-gene regulatory region significantly increased episomal ICE Trb-1 copies (70). The phenotypic advantage of harboring ICE Trb-1 has not been identified; thus, whether *lvrC* also regulates ICE Trb-1 cargo genes remains to be determined.

Because paralogs of the known pluripotent regulator *csrA* are found in many *L. pneumophila* ICEs, and some ICEs – such as SXT, ICEBs1, and ICEclc discussed above – exhibit tight and reciprocal control, we sought to determine whether ICE *csrA* paralogs regulate their own core or cargo activities and competitive host traits. Given the observation that the *lvrC* locus represses ICE Trb-1 mobility and the canonical CsrA represses the core Dot/Icm T4SS, we postulated that *csrA* paralogs function as repressors of ICE traits. Indeed, we demonstrate here co-inheritance of specific *csrA* paralogs with specific T4SS families encoded by ICEs. Using ectopic expression plasmids and the ICE-βox *csrA* paralog *csrT* as a model system, we show CsrT represses the oxidative stress resistance conferred by ICE-βox. In addition, CsrT expression in *L. pneumophila* or *B. subtilis* inhibited motility, a broadly conserved chromosomal pathway predicted to interfere with conjugation.

Experimental Procedures

Bacterial strains, culture conditions and reagents

Legionella pneumophila strains were cultured in *N*-(2-acetamido)-2-aminoethanesulfonic acid (ACES; Sigma)-buffered yeast extract (AYE) broth supplemented with 100 *μ*g/ml thymidine (Sigma) (AYET) at 37°C. Colony forming units (CFU) were identified by plating on ACES-buffered charcoal yeast extract agar (CYE) supplemented with thymidine (CYET) and incubated at 37°C for four days (114). Bacteria cultured overnight in AYET were diluted and grown overnight to obtain cells in exponential (E; OD_{600} = 1.2 to 1.8) or post exponential (PE; OD_{600} = 2 to 3.7) phases. When necessary for mutant or plasmid selection, the following antibiotics were added at the given concentrations: gentamicin (Gibco) at 10μg/mL; chloramphenicol (Fisher) at 5μg/mL. Isopropyl β-D-1-thiogalactopyranoside (IPTG) was purchased from goldbio.com and added to a final concentration of 200μM unless otherwise indicated. Hydrogen peroxide (Sigma) was diluted in AYET and used at a concentration of 2mM. Strains, plasmids, and primers used in this study are summarized in Table 3.1.

Phylogeny and alignment

The predicted amino acid sequences of the 34 ICE-associated *csrA* paralogs (Table 3.2) were aligned using ClustalW2 (115). The alignment was used to generate a maximum likelihood phylogenetic tree with phyML using the LG substitution model, 4 substitution rate categories, and 100 bootstraps (116). The resulting tree was visualized using iTOL (117).

Using the order of *csrA* paralogs determined from the phylogeny, pairwise alignment of the T4SSs were generated using tBLASTx and EasyFig (118). Nucleotide sequences of the T4SS and annotation were taken directly from the NCBI Nucleotide database (Table 3.3).

Table 3.1. Strains, plasmids, and primers used in Chapter Three

Strains

Strain number	Name	Description	Source
E. coli			
MB1001	DH5α	F-endA1 *hsdR17* (r- m+) *supE44 thi-1 recA1 gyrA* (Nal^r) relA1 Δ(lacZYA-argF)$_{U169}$Φ80dLacZΔM15λpirRK6	Lab collection
MB1380	DH5α pcsrT		This study
MB1214	DH5α p206gent		(50)
L.pneumophila			
MB110	Lp02	Philadelphia-1 Str^r $HsdR^-$ Thy^-, wild-type strain for this study	(119)
MB1353	Lp02 ICE-βox::cam	MB110 with ICE-βox marked with camR cassette	(97)
MB370	JR32	Philadelphia-1 Sm^r r^- m^+	(120)
MB1355	JR32+ICE-βox::cam	MB370 with ICE-βox marked with camR cassette	(97)
MB1383	Lp02 pcsrT	MB110 with IPTG-inducible *csrT*; referred to in paper as “donor” (except figure 2)	This study
MB1391	Lp02 ICE-βox::cam	MB1353 with IPTG-inducible *csrT*; “donor” in figure 2	This study

	pcsrT		
MB1384	JR32 pcsrT	MB370 with IPTG-inducible *csrT*; referred to in paper as “recipient”	This study
MB1385	JR32+ICE-βox::cam pcsrT	MB1355 with IPTG-inducible *csrT*; referred to in paper as “transconjugant”	This study
MB1389	Lp02 pcsrA	MB110 with IPTG-inducible *csrA*	This study
MB1390	Lp02 Δ*flaA*	Lp02 *flaA* deletion mutant	Lab collection
B. subtilis			
3610	Wild type		
DS6530	Δ*fliW sow3*	3610 with *fliW* deletion and a point mutation in the *hag* leader sequence, making it insensitive to CsrA repression of motility	(121)
DS4940	*amyE::*$P_{hyspank}$*-csrABs spec*	3610 with IPTG-inducible *B. subtilis csrA*	(121)
DK675	*amyE::*$P_{hyspank}$*-csrALp spec*	3610 with IPTG-inducible *L. pneumophila csrA*	This study
DK676	*amyE::*$P_{hyspank}$*-csrR spec*	3610 with IPTG-inducible *L. pneumophila csrR*	This study
DK677	*amyE::*$P_{hyspank}$*-csrA-T spec*	3610 with IPTG-inducible *L. pneumophila csrT*	This study

DK678	*amyE::P*$_{hyspank}$-*csrA-22 spec*	3610 with IPTG-inducible *L. pneumophila csrA-22 (lpg1003)*	This study
DK679	*amyE::P*$_{hyspank}$-*lvrC spec*	3610 with IPTG-inducible *L. pneumophila LvrC (lpg1257)*	This study
DK1469	*ΔfliWcsrA amyE::P*$_{hyspank}$-*csrABs spec*	DS6530 mutant with IPTG-inducible *B. subtilis csrA*	This study
DK1470	*ΔfliWcsrA amyE::P*$_{hyspank}$-*csrALp spec*	DS6530 with IPTG-inducible *L. pneumophila csrA*	This study
DK1471	*ΔfliWcsrA amyE::P*$_{hyspank}$-*csrT spec*	DS6530 with IPTG-inducible *L. pneumophila csrT*	This study
DK1472	*ΔfliWcsrA amyE::P*$_{hyspank}$-*lvrC spec*	DS6530 with IPTG-inducible *L. pneumophila lvrC (lpg1257)*	This study

Plasmids

Plasmid	Description	Source
p206gent	pMMB66EH derivative, Δ*mob, lacI*^{q}, $P_{taclacUV5}$, gent^{R}	(50)
pcsrA	p206gent with *csrA* with 6x-His epitope ligated into the SalI and HindIII sites, IPTG-inducible *cs*	Abbott 2015, in review

pcsrT	p206gent with *csrT* with 6x-his epitope ligated into the SalI and HindIII sites, IPTG-inducible *csr*	This study

Primers

Number	description	sequence	Source
ZA11	Fwd SalI *csrT*	GTCGACCTGAAGTGGCTAAAACCCAATTAC	This study
ZA12	Rev HindIII-6x his-*csrT*	AAGCTTTTAATGATGATGATGATGATGATGGTGATTGAGGATTGATTGCT	This study
ZA33	SalI *csrA*-his fwd	GTCGACGGAAGCGTTCTATGGAGAAGTAGG	Abbott 2015, in review
ZA34	HindIII *csrA*-his rev	AAGCTTTTAATGATGATGATGATGATGTACTGCTTGTTCCGAATCATCAG	Abbott 2015, in review
KF152	*lpg2112* fwd	CACTGGAAGCCTACATTGGG	This study
KF153	*lpg2112*rev	CCATTATAACCTGCTGAGACC	This study
KF160	*lpg2098* fwd	GGTTTTGTACTGTTGGGTCG	This study
KF161	*lpg2098* rev	CTATGATGGTGGTACTGAGCC	This study

KF162	*lpg2100* fwd	GTGATACCCGCACTGTGG	This study
KF163	*lpg2100* rev	CAAACACAACACCCACCTC	This study
SL1	16S fwd	AGAAGGCCTGAGGGTTGTAAAGCA	lab collection
SL2	16S rev	ACCCTTTACGCCCAGTAATTCCGA	lab collection
3170	*amyE* fwd	GGTGGAAACGAGGTCATCATTTC	This study
3177	Spectinomycin fwd	CTAATTCAAGGCGTGTCTCAC	(122)
3180	*amyE* rev	GCGGTATTCCGTATGTCAAG	(122)
3519	Spectinomycin rev	CACTCTACCTCCTGCTAGCT	This study
3520	*csrALp* fwd	AGCTAGCAGGAGGTAGAGTGATGTTGATTTTGACTCGGCGT	This study
3521	*csrALp* rev	ATGATGACCTCGTTTCCACCAGTTCCCACAGCTTATATTAATT	This study
3524	*csrT* fwd	AGCTAGCAGGAGGTAGAGTGATGTTGAGTTTAACTAGAAGAGT	This study
3525	*csrT* rev	ATGATGACCTCGTTTCCACCTTAGAAAAATAGCCATCGCCC	This study
3526	*csrA-22* fwd	AGCTAGCAGGAGGTAGAGTGATGCTGATCCTAGACCGCAA	This

			study
3527	*csrA-22* rev	ATGATGACCTCGTTTCCACCCGTCGGCTATAGTTAAAGGAC	This study
3528	*lvrC* fwd	AGCTAGCAGGAGGTAGAGTGATGTTGGTTTTAACACGAAAAGC	This study
3529	*lvrC* rev	ATGATGACCTCGTTTCCACCGGGCTTATTTCCAAATCGCTC	This study

Table 3.2. *csrA* paralogs in *Legionellae* ICEs

Gene	Species	Strain	Amino acid sequence
lpep00046	*L. pneumophila*	LPE509	MLILTRRIGETVVIGDDVFITILGIKGNQIRLGFDAPDHVSIHRQEIYLKVQEQKKMRLDSGEAVNGNGMLITPLKQTEPHQYTAH
lpc0169	*L. pneumophila*	Corby	MLVLTRRVGESVVIHDDVYCTIVGYRDGEVRLAFDAPRSIPVHRDEIQRRIHRARIKDNWFIDKAANKESIVDRLINKFKNSTSAVKA
lpa00223	*L. pneumophila*	Alcoy	MLVLTRRVGESVVIHDDVYCTIVGYRDGEVRLAFDAPRSIPVHRDEIQRRIHRARIKDNWFIDKAANKESIVDRLINKFKNSTSAVKA
lpc2813	*L. pneumophila*	Corby	MLVLTRRVGESVVISEDIYCTIVGYQNDEVRLAFDAPKSIPIHRDEIQRRIYRDQIKDNKFVDKAANNESIVDRLINKFKSSASPTNS
lpa00796	*L. pneumophila*	Alcoy	MLVLTRRVGESVVISEDIYCTIVGYQNDEVRLAFDAPKSIPIHRDEIQRRIYRDQIKDNKFVDKAANNESIVDRLINKFKSSASPTNS
lpo2456	*L. pneumophila*	Lorraine	MLVLTRKVGESVVISEEVYCTVVGYRDGEVRLAFDAPQSIPVHRDEIQRRIYRERQRDQWFNDSPSNKENIVDRLISKFKNGLKSA
lpe01074	*L. pneumop*	LPE509	MLVLTRKVGESVVISEEVYCTVVGYRDGEVRLAFDAPQSIPVHRDEIQRRIYRER

	hila		QKDQWFSDSPSNKESIIDRLISKFKHGL KSA
llo2874	*L. longbeachae*	NSW150	MLVLTRKIGESVVISEDIYCTVVGYRDGE VRLGFDAPQSIPIHRDEIQRRIYRERQKD QSFNDSPPHKKSIVDRLISKFKHELKSA
plpl0012	*L. pneumophila*	Lens	MLILERRVGETVAIENKVFCMVLDHQLD GQLKLAFDAPECVPFHRFEIQEGS
plpp0016	*L. pneumophila*	Paris	MLILTRRVGDTVVIGNEVFCTVLEQQHD GQIKLAFDAPKSIPIHRFEIQKQIMQKIIE GTYTNDVAWNETVIERLTSQFNRVSHW N
lpop0154	*L. pneumophila*	Lorraine	MLILTRRIGETVLINDDIYITVLGVKGNQV RLGFDAPQDVIIHRQEIHQKIKKEQSLFL NKPGQWKEARGVQTH
lpg2094	*L. pneumophila*	Philadelphia-1	MLSLTRRVGESIVIGEDIFITVLCCKGNQ VRIGFNAPNSVAIHRYEIYQKIQSEKHDG LADPTKKFCPSMQQSILNHH
lpe01011	*L. pneumophila*	LPE509	MLSLTRRVGESIVIGEDIFITVLCCKGNQ VRIGFNAPNSVAIHRYEIYQKIQSEKHDG LADPTKKFCPSMQQSILNHH
lp12_2035	*L. pneumophila*	ATCC 43290	MLSLTRRVGESIVIGEDIFITVLCCKGNQ VRIGFNAPNSVAIHRYEIYQKIQSEKHDG LADPTKKFCPSMQQSILNHH
lpp1074	*L. pneumophila*	Paris	MLTLIRRIGEAIYIDKGRIKVHLISEKEGLI RLGIEAPKHVDIERKEVFVRKAVAQHEQ

	hila		AQALRNQSGGDDA
lp12_1033	*L. pneumophila*	ATCC 43290	MLTLIRRIGEAIYIDKGRIKVHLISEKEGLI RLGIEAPKHVDIERKEVFVRKAVAQHEQ AQALRNQSGGDDA
lpo2781	*L. pneumophila*	Lorraine	MLILIRRMGEAIYIDKGRIKVLLISEKEGLI KLGIDAPKHIDVERKEVFIQKAMEQHAL AQKLRDKSTESGGNHA
lpg1003	*L. pneumophila*	Philadelphia-1	MLILDRKIGEEIYINKGKIKITVLYEKNGLI GIGVRAPSEIDIDRKEVFIRKYIQKLDQE NKSNQG
lpl1036	*L. pneumophila*	Lens	MLILDRKIGEEIYINKGKIKITVLYEKNGLI GIGVRASSEIDIDRKEVFIRKYIQKLDQE NKSNQG
lpc2276	*L. pneumophila*	Corby	MLILDRKIGEEIFINKGKIKITVLYEKNGLI GIGVRAPSEIDIDRKEVFIRKYIQKLDQE NKPNQE
lpa01531	*L. pneumophila*	Alcoy	MLILDRKIGEEIYINKGKIKITVLYEKNGLI GIGVRASSEIDIDRKEVFIRKYIQKLDQE NKSNQG
lpv1151	*L. pneumophila*	HL060410 35	MLILDRKIGEEIYINKGKIKITVLYEKNGLI GIGVRAPSEIDIDRKEVFIRKYIQKLDQE NKSNQG
lpe02190	*L. pneumophila*	LPE509	MLILDRKIGEEIYINKGKIKITVLYEKNGLI GIGVRAPSEIDIDRKEVFIRKYIQKLDQE NKSNQG

lpp2378	*L. pneumophila*	Paris	MLVLTRKKGEQIVIDKGQIEIHVIYQRRG VVALGIKAPAHIDVDRKEIFLRKQTNPQN NDKEISK
lpc1860	*L. pneumophila*	Corby	MLVLTRKKGEQILIDKGQIEIHVIYQRRG VVALGIKAPAHIDVDRKEIFLRKQTNPQN TNIEEPK
lpv1819	*L. pneumophila*	HL060410 35	MLVLTRKKGEQILIDKGQIEIHVIYQRRG VVALGIKAPAHIDVDRKEIFLRKQTNPQN TDIEEPK
lp12_2077	*L. pneumophila*	ATCC 43290	MMLVLTRKKGEQILIDKGQIEIHVIYQRR GVVALGIKAPAHIDVDRKEIFLRKQTNP QNTNIEEPK
llb1171	*L. longbeachae*	D-4968	MLVLTRRVGEQIFIDKGQIQIKVLFVRNG NIALGIQAPPNVDVDREEIYYLKKEGIIVE SN
lpg1257	*L. pneumophila*	Philadelphia-1	MLVLTRKAGQQILIGKGLIQMKVLKVDD DIISIGIKAPQHIDIDREEIYLKKLQQEQAE SSMQKVAP
lpl0150	*L. pneumophila*	Lens	MLVLTRKAGQQILIGKGLIQMKVLKVDD DIISIGIKAPQHIDIDREEIYLKKLQQEQAE SSMQKVAP
lpv0167	*L. pneumophila*	HL060410 35	MLVLTRKAGQQILIGKGLIQMKVLKVDD DIISIGIKAPQHIDIDREEIYLKKLQQEQAE SSMQKVAP
lpp0168	*L. pneumop*	Paris	MLVLTRKAGQQILIGKGLIQMKVLKVEN DIISIGIKAPSHIDIDREEIYFRKLRQEQEA

	hila		ANDAEMAI
	L. longbeach		MLILSRKIGENVLIDQGTIQIKLLDVKGRY ARIGFIAPAGTDIDREEIYIRKKQSRDLN
llb1138	*ae*	D-4968	KKAANHEVNN
	L. longbeach		MLVLERKIGQKVVIDNGAIEVKVLKPHG DMIRLGFKAPQNMDINKEEIYLRKVLQV
llo1850	*ae*	NSW150	PEFLKPVVRNHETRRRK

Each gene is listed with its locus tag and inferred amino acid sequence.

Table 3.3. Summary of ICEs from Figure 3.1B.

***csr* gene marking ICE**	**Strain**	**Accession number**	**5' T4SS coordinate**	**3' T4SS coordinate**	**T4SS lineage (color in Figure 1B)**
lpc0169	*L. pneumophila* Corby	CP000675.2	184300	200451	Trb (blue)
lpa00223	*L. pneumophila* Alcoy	CP001828.1	184068	200219	Trb (blue)
lpc2813	*L. pneumophila* Corby	CP000675.2	617842	633964	Trb (blue)
lpa00796	*L. pneumophila* Alcoy	CP001828.1	613023	629145	Trb (blue)
lpo2456	*L. pneumophila* Lorraine	FQ958210.1	2581394	2597460	Trb (blue)
lpe01074	*L. pneumophila* LPE509	CP003885.1	1109051	1125125	Trb (blue)
llo2874	*L. longbeachae*	FN650140.1	3355412	3372833	Trb (blue)

	NSW150				
lpg2094	*L. pneumophila* Philadeliphia-1	AE017354.1	2319208	2344884	Tra (red)
lpe01011	*L. pneumophila* LPE509	CP003885.1	1051761	1068953	Tra (red)
lp12_2035	*L. pneumophila* ATCC 43290	CP003192.1	2243991	2261276	Tra (red)
lpop0154	*L. pneumophila* Lorraine	FQ958212.1	122878	142676	Diverse (purple)
lpep00046	*L. pneumophila* LPE509	CP003886.1	19244	40410	Diverse (purple)
plpp0016	*L. pneumophila* Paris	CR628338.1	13345	42715	Diverse (purple)
plpl0012	*L. pneumophila* Lens	CR628339.1	10787	28932	Diverse (purple)
llo1850	*L. longbeachae* NSW150	FN650140.1	2164094	2181119	Diverse (purple)

llb1138	*L. longbeachae* D-4968	ACZG01000001.1	1196029	1211847	Lvh (yellow)
lpp0168	*L. pneumophila* Paris	CR628336.1	194054	210931	Lvh (yellow)
lpg1257	*L. pneumophila* Philadelphia-1	AE017354.1	1368713	1386591	Lvh (yellow)
lpl0150	*L. pneumophila* Lens	CR628337.1	181867	201513	Lvh (yellow)
lpv0167	*L. pneumophila* HL06041035	FQ958211.1	181295	198468	Lvh (yellow)
llb1171	*L. longbeachae* D-4968	ACZG01000001.1	1236013	1254272	Lgi (green)
lpc1860	*L. pneumophila* Corby	CP000675.2	2808352	2826507	Lgi (green)
lp12_2077	*L. pneumophila* ATCC 43290	CP003192.1	2296777	2314983	Lgi (green)
lpp2378	*L.*	CR628336.1	2726191	2744349	Lgi

	pneumophila Paris				(green)
lpv1819	*L. pneumophila* HL06041035	FQ958211.1	1840909	1859070	Lgi (green)
lpo2781	*L. pneumophila* Lorraine	FQ958210.1	2899570	2917401	Lgi (green)
lp12_1033	*L. pneumophila* ATCC 43290	CP003192.1	1101878	1119680	Lgi (green)
lpp1074	*L. pneumophila* Paris	CR628336.1	1177462	1195264	Lgi (green)
lpv1151	*L. pneumophila* HL06041035	FQ958211.1	1140510	1158271	Lgi (green)
lpg1003	*L. pneumophila* Philadelphia-1	AE017354.1	1076121	1093906	Lgi (green)
lpe02190	*L. pneumophila* LPE509	CP003885.1	2334332	2352138	Lgi (green)
lpc2276	*L. pneumophila*	CP000675.2	1189397	1207218	Lgi (green)

	Corby				
lpl1036	*L. pneumophila* Lens	CR628337.1	1149440	1167201	Lgi (green)
lpa01531	*L. pneumophila* Alcoy	CP001828.1	1185994	1203755	Lgi (green)

Sequence identification for the T4SSs aligned in Figure 3.1B, listed in the same order as they are aligned.

Induced expression constructs

Wild-type *csrA* and *csrT* with C-terminal 6x-Histidine tags were amplified from Lp02 genomic DNA using primer sets ZA33+34 and ZA11+12, respectively. The resultant PCR products were digested with *Sal*I and *Hind*III and ligated into p206gent (50). These plasmids were then electroporated into Lp02 to generate strains MB1389 and MB1383. We verified that adding 200μM IPTG resulted in protein expression by performing western blots using a 1:5000 dilution of anti-His(C-term)-HRP conjugated antibody following the western blot protocol described below (data not shown).

Mice

Six- to eight-week-old female A/J mice were purchased from Jackson Laboratories. Mice were housed in the University Laboratory Animal Medicine Facility at the University of Michigan Medical School under specific-pathogen-free conditions. The University Committee on Use and Care of Animals approved all experiments conducted in this study.

Hydrogen peroxide exposure assay

Stress resistance was assessed by quantifying bacterial CFU after exposure to hydrogen peroxide. E phase strains containing pcsrT (MB1383, MB1384, MB1385) or pcsrA (MB1389) as a control were cultured in AYET with or without IPTG induction

overnight. After subculture to OD_{600} = 1.0, cultures were treated with 2 mM H_2O_2 for 1 h at 37°C. Mean +/- SEM percent survival was calculated from triplicate samples.

Quantitative PCR

ICE-βox cargo gene expression was probed using quantitative Real-Time PCR (qRT-PCR). RNA from strain MB1383 cultured to E phase with or without 200μM IPTG was isolated using TRIZol reagent (Life Technologies) and its quality assessed using an Agilent Bioanalyzer 2100 according to manufacturer's protocol. Primer pairs KF162+163, KF152+153, and KF160+161 were used to quantify cargo gene expression in IPTG-induced RNA pools (*lpg2100, lpg2112 magA*, *lpg2098 msrA3*, respectively) relative to uninduced. As an internal control, chromosomal 16S rRNA levels were used to normalize input RNA levels using primer pair SL1+2. Log_2-transformed values of the mean ± standard error of the mean (SEM) fold change #(induced – uninduced) amplicons calculated from three independent experiments performed in triplicate are presented.

Intracellular growth and immunofluorescence microscopy

Growth of bacteria in bone marrow-derived macrophages from A/J mice (Jackson Laboratories) was assessed as described previously (75). Strains were cultured to PE phase with or without 200μM IPTG overnight prior to infection. To account for infectivity

differences, uninduced motile strains were infected at an MOI of 1 while induced nonmotile strains were infected at an MOI of 2. IPTG was included in the infection medium of induced strains at a concentration of 1mM as described previously (110). Infection efficiency was quantified as the % CFU of bacteria associated with macrophages at 90' post infection relative to input titer. Microscopy was performed by plating 3 x 10^5 macrophages on 12-mm glass coverslips overnight prior to infection with bacteria cultured as described above. At 90' post infection, macrophages were fixed and stained as described previously (123) using a 1:50 dilution of *L. pneumophila* primary antibody obtained from mouse monoclonal hybridoma cell line CRL-1765 (ATCC) and a 1:1000 dilution of anti-mouse IgG antibody conjugated to Oregon Green (Molecular Probes). The DNA stain DAPI (4′,6-diamidino-2-phenylindole) was purchased as ProLong Gold antifade reagent (Molecular Probes) and included in the mounting medium. NADPH oxidase experiments were performed using a pair of cell lines J774.16 (WT) and J774.D9 *phox* (deficient in gp91 subunit of NADPH oxidase) that were infected as described above (124).

Conjugation

To analyze ICE-βox transfer by conjugation, the thymidine auxotroph donor Lp02 strain containing a chloramphenicol-resistance marked ICE-βox and pcsrT (MB1391) were cultured with or without IPTG overnight to E phase, and the thymidine prototroph recipient JR32 (MB370) was also grown overnight to E phase. 10^9 donor cells were

mixed with 10^{10} recipient cells on 0.22-μm filters (Millipore) placed on prewarmed CYET agar plates and incubated for 2 h at 37°C as described previously (97, 125). For induced strains, 10 μl of 200mM IPTG was placed under the filter. Serial dilutions of the mating mixture were plated on CYET-cam (5μg/ml) to select for donors and CYE-cam to select for transconjugants. Transconjugation efficiency was calculated as CFU transconjugants/CFU donor cells in triplicate from three independent experiments.

Motility and flagellin western blot

Wild-type (MB110), Δ*flaA* mutant (MB1390), and strains carrying pcsrA and pcsrT (MB1389 and MB1383) were cultured in AYET to E-phase and then diluted to OD_{600} = 0.2. Cultures of strains MB1389 and MB1383 were split into two tubes, and one was induced with 200μM IPTG. Cultures were then incubated at 37°C for ~15 h to PE phase, and then motility was assessed qualitatively by observation of wet mounts by inverted phase microscopy. Aliquots of the cultures were subsequently normalized to OD_{600} = 10, and then resuspended in 100μL Laemmli buffer (2% SDS, 10% glycerol, 5% 2-mercaptoethanol, 0.005% bromophenol blue, 62.5mM Tris-HCl, pH 6.8). Samples were then lysed by boiling for 5 min, and debris pelleted at 13,000 rpm for 2 min. Proteins were separated on a 12% mini-PROTEAN TGX precast gel (Bio-Rad), and Precision Plus Kaleidoscope Protein Standard ladder (Bio-Rad) was used as a size marker and to verify transfer. To verify equal loading and transfer of each sample, Ponceau S (Fisher) staining was performed on a duplicate membrane. Flagellin was

detected using a 1:100 dilution of 2A5 rabbit monoclonal antibody (Gift from NC Engelberg, UMMS), 1:3000 goat anti-rabbit secondary IgG-HRP (Pierce), and the SuperSignal West Pico Chemiluminescent Substrate (Thermo Scientific).

B. subtilis growth conditions

Bacillus subtilis strains were cultured in Luria-Bertani (LB) (10 g tryptone, 5 g yeast extract, 5 g NaCl per L) broth or on LB plates fortified with 1.5% Bacto agar at 37˚C. When appropriate, antibiotics were included at the following concentrations: 10 μg/ml tetracycline, 100 μg/ml spectinomycin, 5 μg/ml chloramphenicol, 5 μg/ml kanamycin, and 1 μg/ml erythromycin plus 25 μg/ml lincomycin. 1mM IPTG (Sigma) was added to the medium when appropriate.

B. subtilis strain construction

To generate the *amyE::*$P_{hyspank}$*-csrALp* spec complementation construct, PCR product containing the *csrALp* coding region was amplified from *L. pneumophila* chromosomal DNA using the primer pair 3520/3521. DNA fragments containing the IPTG-inducible $P_{hyspank}$ promoter, a spectinomycin resistance cassette and the *amyE* region were amplified from the strain DS4940 as template using primers 3177/3519 and 3170/3180. Next, the PCR products were ligated using Gibson assembly (126). The complementation constructs *amyE::*$P_{hyspank}$*-csrX* spec, *amyE::*$P_{hyspank}$*-csrT* spec,

amyE::P$_{hyspank}$*-csrA-22* spec, and *amyE::P*$_{hyspank}$*-lvrC* spec were generated in a similar way using PCR amplicons from *L. pneumophila* chromosomal DNA using the primer pairs 3522/3523, 3524/3525, 3526/3527, and 3528/3529 respectively.

All constructs were first introduced into the domesticated strain DS2569 by natural competence and then transferred to the 3610 and DS6530 background using SPP1-mediated generalized phage transduction (127).

B. subtilis swarm expansion assay

Cells were cultured to mid-log phase at 37˚C in LB and resuspended to OD_{600} = 10 in pH 8.0 PBS buffer (137 mM NaCl, 2.7 mM KCl, 10 mM Na_2HPO_4, and 2 mM KH_2PO_4) pH 8.0, containing 0.5% India ink (Higgins). Freshly prepared LB containing 0.7% Bacto agar (25 ml/plate) was dried for 20 min in a laminar flow hood, centrally inoculated with 10 μl of the cell suspension, dried for another 10 min, and incubated at 37˚C. The India ink demarks the origin of the colony, and the swarm radius was measured relative to the origin. For consistency, an axis was drawn on the back of the plate and swarm radii measurements were taken along this transect. For experiments including IPTG, cells were propagated in broth in the presence of IPTG, and IPTG was included in the swarm agar plates.

Results

csrA paralogs and their associated T4SSs are genetically linked

The *Legionella* pan-genome has been predicted or demonstrated to encode many ICEs (74, 97, 128). In each of the 34 legionellae ICEs identified (Table 3.3), a *csrA*-like gene immediately precedes the locus encoding the T4SS. Previously we identified distinct families of *csrA*-like genes based on their amino acid sequence similarity (Abbott 2015, in review). Likewise, *Legionella* genomic islands encode several different lineages of T4SSs (69, 70, 97, 128, 129). Therefore, we investigated whether particular lineages of ICE-encoded T4SS were genetically linked to a distinct *csrA* paralog. To do so, we first determined the relationship of all 34 *csrA* paralogs by generating a phylogenetic tree. Four distinct groups were apparent based on their amino acid sequence; only five of the 34 paralogs did not clearly fall into any group (Figure 3.1A).

To determine if the T4SS lineages paired with a specific group of *csrA*-paralogs, we next aligned the T4SSs associated with each of the *csrA* paralogs. Indeed, within each *csrA*-paralog group, the associated T4SSs lineages were quite similar, whereas there was little similarity between T4SSs that are genetically linked to different *csrA* families (Figure 1B). For instance, all the T4SSs associated with *csrA*-paralogs in group IV aligned strongly and indeed included every T4SS in the LGI lineage identified by Wee et al. (128). On the other hand, the T4SS in *csrA* group IV did not align with those of the Lvh T4SS lineage (129), the Trb T4SS lineage (69), or the Tra T4SS lineage (97).

However, although the *csrA* paralogs were genetically linked to their T4SSs, the same relationship did not exist between *csrA* paralogs and associated cargo regions (data not shown). The linkage of particular groups of *csrA*-paralogs with specific T4SS lineages suggests selective pressure minimizes genetic drift between the *csrA* paralog and its associated T4SS locus. Accordingly, we postulated that there is a functional relationship between each ICE regulator and the genes that encode its conjugation machinery.

csrT inhibits ICE-βox transfer

The genetic linkage between ICE-encoded *csrA* paralogs and their adjacent T4SS loci appears to be maintained by selective pressure, and ICE conjugation is mediated by its T4SS (70, 130). Therefore, we hypothesized that ICE transfer is regulated by ICE *csrA* genes, paralogs of the pluripotent *L. pneumophila* regulator CsrA. ICE-βox of *L. pneumophila* Philadelphia-1 carries the *csrA* paralog *lpg2094*, which we name here *csrT* (csrA paralog for ICE transfer) (97). To test if ectopic expression of *csrT* is sufficient to regulate ICE-βox conjugative transfer, we created a plasmid (pcsrT) on which *csrT* transcription is induced by IPTG. To create a donor strain, we transformed Lp02 by electroporation with plasmid pcsrT. Lp02 is a lab derivative of the Philadelphia-1 strain that contains ICE-βox that has been marked with a chloramphenicol resistance cassette (97). Donor cells cultured with or without IPTG were mated with the recipient strain JR32, a lab derivative of Philadelphia-1 that does not contain ICE-βox (97). Indeed, ectopic expression of *csrT* in laboratory conditions repressed conjugative

transfer of ICE-βox, as transconjugation efficiency was reduced ~10 fold ($p < 0.05$) compared to donors that were not induced to express *csrT* (Figure 3.2). *csrT* repression of ICE-βox conjugation is consistent with the hypothesis that the *csrA* paralogs regulate their T4SSs, as predicted by their genetic relationship (Figure 3.1) and the repression of ICE-Trb1 excision by the *lvrC* locus (70).

ICE-βox excision is not sensitive to ectopic *csrT* expression

Conjugative transfer requires that ICEs first direct their own excision from the host chromosome (131). Because ectopic *csrT* expression reduces ICE-βox conjugation and the locus encoding another *csrA* paralog, *lvrC*, inhibits excision of its own ICE Trb-1 (70), we tested if *csrT* expression also represses ICE-βox excision. To quantify excised and integrated copies of ICE-βox, quantitative PCR using specific primers was performed as described previously (97) using template DNA isolated from donor cells cultured to E and PE growth phases with or without ITPG. ICE-βox excision was not affected by ectopic expression of *csrT* in either growth phase. Therefore, in the conditions tested ectopic expression of *csrT* mediates transconjugation repression downstream of ICE-βox excision.

***csrT* represses *L. pneumophila* resistance to hydrogen peroxide conferred by ICE-βox**

We postulated that CsrT inhibits the ICE-βox T4SS, based on three independent observations. ICE-encoded *csrA* paralogs are genetically linked with their associated

Figure 3.1. Relationship of CsrA paralogs and T4SSs.

(A) To determine the relationship between 34 ICE-associated *csrA* loci, a maximum likelihood phylogenetic tree was generated from their predicted amino acid sequences. Four distinct clusters are boxed in blue, red, yellow, and green. The five protein sequences that did not clearly fall into any cluster are boxed in purple. Branches with at least 60% support from 100 bootstraps are labeled.

(B) Pairwise translated nucleotide sequence identity (tBLASTx) of 34 T4SSs in the legionellae pan-genome was performed based on the relationship of their adjacent *csrA* paralogs as determined by the phylogeny in (A). *lvrA/B* genes are teal arrows; *csrA* paralogs are black arrows and indicated by pointer; T4SSs are colored and labeled by group to correspond with the boxes in (A). Grey bars between T4SS operons indicate the % identity as shown by the scale bar. The bottom two T4SSs from the left column are reproduced as the top two in the right column for continuity.

Figure 3.1. Relationship of CsrA paralogs and T4SSs.

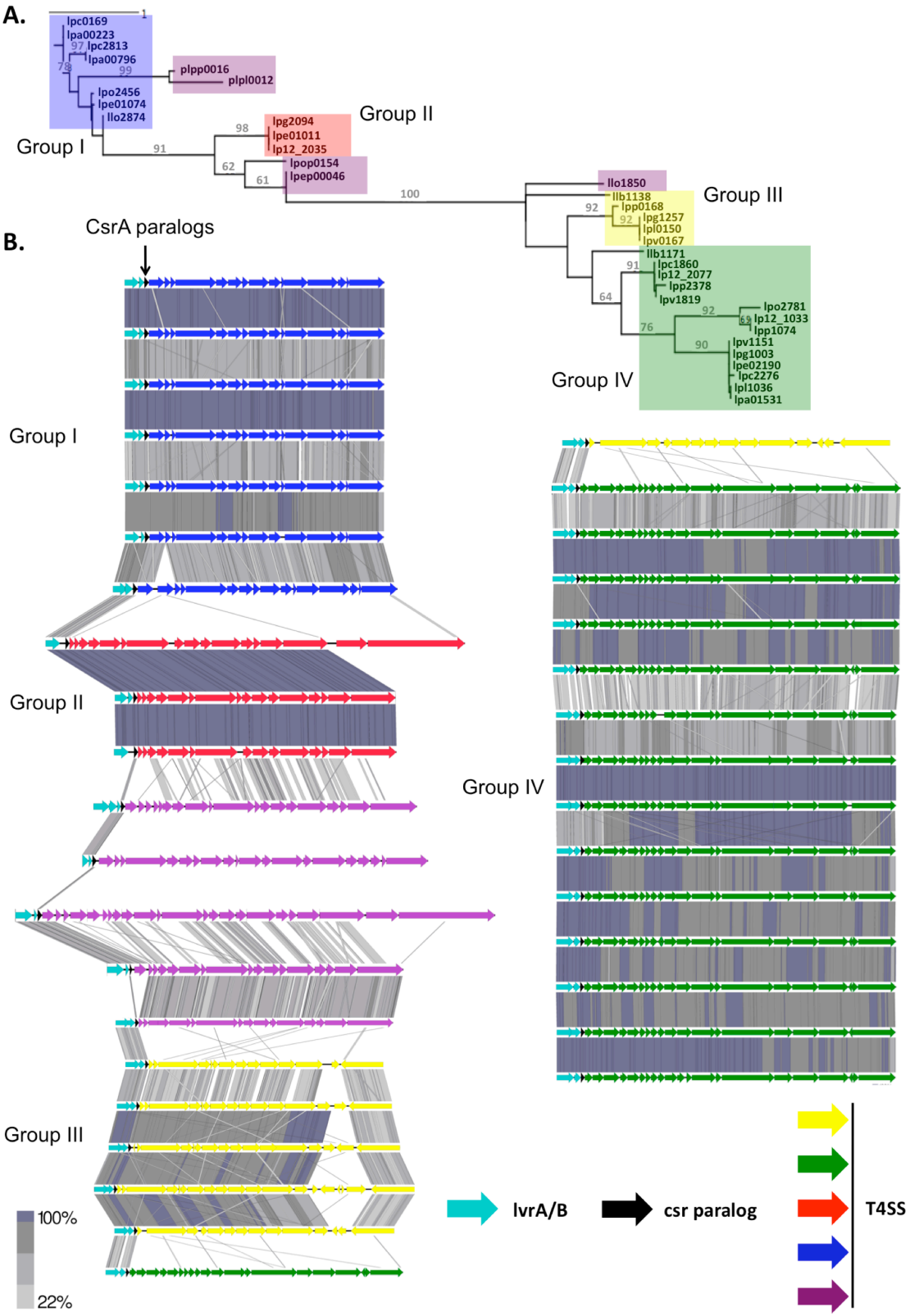

Figure 3.2. Ectopic *csrT* expression reduces ICE-βox transfer.

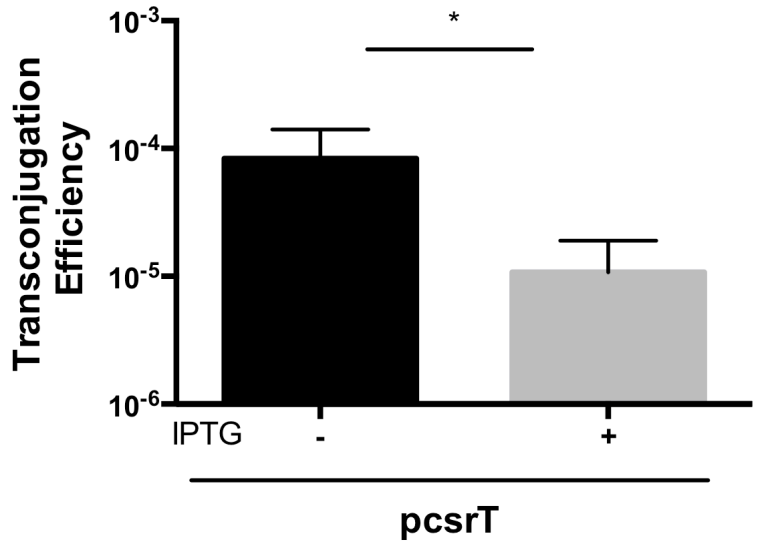

ICE-βox null recipient strain (MB370) was mated with E phase ICE-βox donor strain containing pcsrT (MB1383) after overnight culture with (gray) or without IPTG (black) to induce ectopic expression of CsrT. Mean transconjugation efficiency of ICE-βox is expressed as (CFU transconjugants/ CFU donor) +/- SEM of results from three independent experiments. *T* test indicates the difference between uninduced and induced transconjugation efficiency is statistically significant ($P < 0.05$).

T4SSs (Figure 3.1); ectopic expression of *csrT* reduces ICE-βox conjugation but not excision (Figure 3.2, data not shown); and canonical CsrA inhibits Dot/Icm T4SS-mediated phenotypes, including host vesicular trafficking (111). Therefore, we tested whether CsrT can repress ICE-βox-mediated phenotypes. In *L. pneumophila*, ICE-βox confers resistance to β-lactam antibiotics and oxidative stress, such as from bleach and hydrogen peroxide (97). In particular, we assayed the capacity of ICE-βox to increase *L. pneumophila* resistance to hydrogen peroxide (97) after transforming donor, transconjugant and recipient strains with plasmid pcsrT. As predicted, ectopic *csrT* expression abrogated the protective effects of ICE-βox to 1 h exposure to 2 mM hydrogen peroxide (Figure 3.3A). Donor and transconjugant ICE-positive strains that expressed *csrT* were ~10-fold more susceptible to killing by hydrogen peroxide when compared to the same strains cultured without IPTG-induction of *csrT* ($P < 0.05$, $P < 0.01$). *csrT* repressed *L. pneumophila* resistance to oxidative stress by a mechanism that requires ICE-βox, since the strain that lacked the element was sensitive to hydrogen peroxide whether or not expression of pcsrT was induced with IPTG. Thus, when expressed ectopically, *csrT* inhibits ICE-βox-mediated hydrogen peroxide resistance.

ICE-βox cargo genes encoding oxidative-stress resistance enzymes are not repressed by ectopic *csrT* expression

Figure 3.3: Ectopic *csrT* expression represses oxidative stress resistance conferred by ICE-βox.

A) When expressed ectopically, CsrT abrogates the capacity of ICE-βox to protect *L. pneumophila* from hydrogen peroxide stress. E phase cultures of ICE-βox donor (D, dark grey), naïve recipient (R, white) or ICE-βox transconjugant (T, light gray) strains that contained IPTG-inducible plasmid pcsrT (Strains MB1383, MB1384, and MB1385, respectively) were cultured overnight with (striped) or without (plain) IPTG and then exposed to 2 mM H_2O_2 for 1 h. Mean % survival +/- SEM was calculated from three independent experiments as (CFU post-treatment/CFU pre-treatment)*100. *T* tests indicate statistically significant differences between treated, pcsrT-induced ICE-βox strains and the treated uninduced strains (*, $P < 0.05$, ** $P < 0.01$).

B) ICE-βox cargo transcripts are differentially expressed in *csrT*-induced strains. Expression analysis of three ICE-βox cargo genes – *lpg2100*, *magA*, and *msrA3* – was performed on RNA isolated from E phase ICE-βox donor cells carrying pcsrT (MB 1383) after culture overnight with or without IPTG. qRT-PCR results are expressed as $\log_2$(transcript induced – transcript uninduced) and means +/- SEM of three independent RNA isolates are presented.

C) CsrT induction represses bacterial degradation resistance in macrophages. E and PE phase strain MB110 Lp02 and PE phase strain MB370 JR32 (E, PE, and JR, respectively; hatched bars), ICE-βox donor (D, dark grey), recipient (R, white), or transconjugant (T, light gray) strains containing the inducible pcsrT plasmid (Strains MB1383, MB1384, and MB1385)) that had been cultured overnight with (striped) or without (plain) IPTG, were used to infect A/J macrophages at an MOI of 2 (induced) or 1 (uninduced). At 90' post infection, bacterial integrity was quantified by immunofluorescence microscopy. Presented are the mean % +/- SEM of total bacteria that are intact vs. degraded from three independent experiments. *T* tests indicate that differences between induced and uninduced D and T strains are significant ($P < 0.001$).

D) CsrT induction inhibits efficient infection of macrophages. A/J mouse macrophages were infected as described in (C). At 90' post infection, cells were lysed and CFU enumerated. Percent of infectious bacteria was calculated as (CFU at 90'/CFU of infection input) * 100 and is expressed as mean +/- SEM from three replicates in one experiment representative of three others. *T* test confirms differences between induced and uninduced strains are significant (* $P < 0.005$, *** $P < 0.05$).

Figure 3.3: Ectopic *csrT* expression represses oxidative stress resistance conferred by ICE-βox

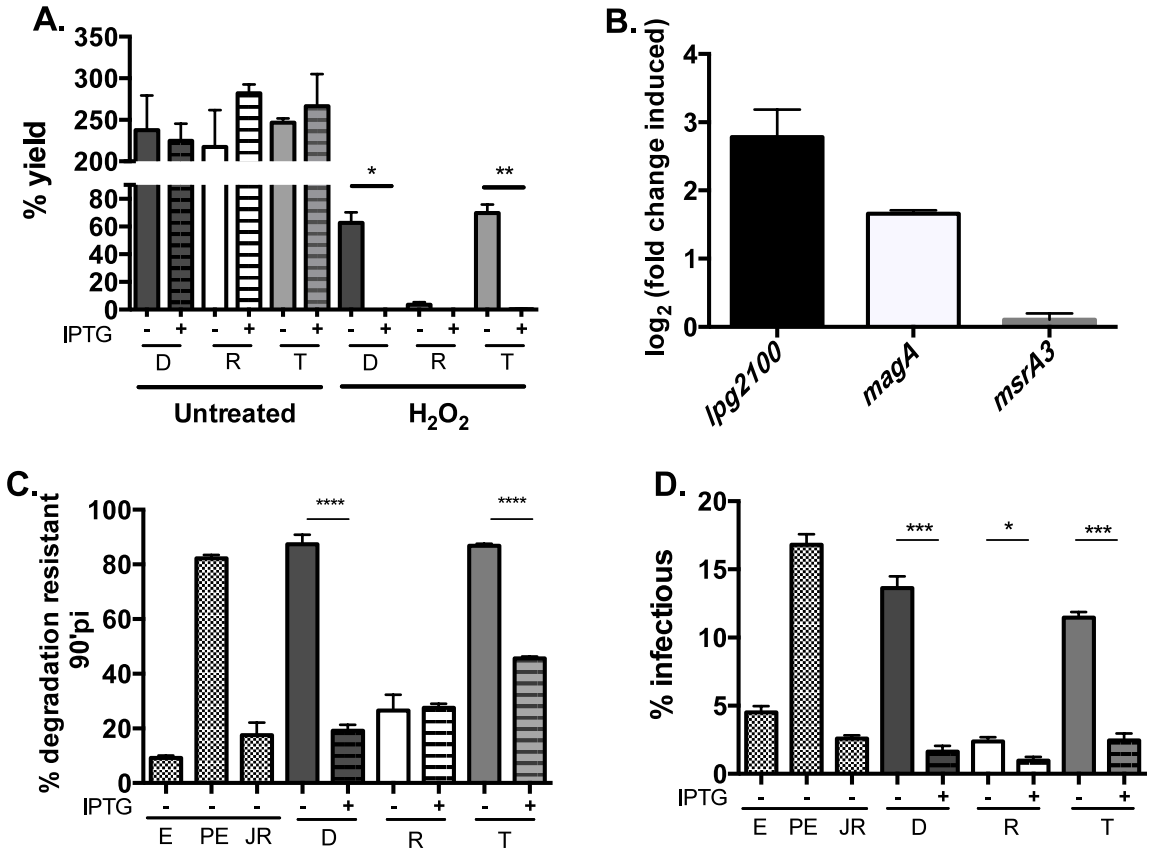

ICE-βox carries 38 putative cargo genes, some of which are predicted to confer resistance to oxidative stress (97). In particular, three operons near the 3' end of the element are homologous to loci in other species that are activated during oxidative stress (97). First, *lpg2100* has sequence homology to genes encoding cytochrome C oxidase, a protein commonly known to reduce hydrogen peroxide as part of the electron transport chain (132). Second, *lpg2112* is a homolog of the alkyl hydroperoxide reductase *magA*, which *Salmonella* species use to scavenge hydrogen peroxide species (89). Third, *Lpg2098* has homology to the methionine sulfoxide reductase gene *msrA3*, which in *E. coli* is protective against hydrogen peroxide-induced death (133). Accordingly, we tested whether *csrT* repression of these cargo genes accounts for its inhibition of ICE-βox-mediated oxidative stress resistance (Fig, 3.3A). To analyze transcript levels of homologs to cytochrome C oxidase (*lpg2100*), alkyl hydroperoxide reductase (*magA*), and methionine sulfoxide reductase (*msrA3*), we analyzed RNA isolated from E phase cultures of ICE-βox donor cells that either did or did not ectopically express *csrT*. In contrast to our hypothesis, in response to *csrT* induction, *lpg2100* was upregulated ~7 fold ($P < 0.001$), *magA* was induced ~2 fold ($P < 0.005$) and *msrA3* transcript levels were unaffected (Figure 3.3B). Therefore, in culture conditions favorable for replication, ectopic expression of *csrT* enhances, rather than represses, transcription of this set of ICE-βox encoded cargo genes. Accordingly, ectopically expressed *csrT* inhibits ICE-βox-mediated oxidative stress resistance (Figure 3.3A) by a mechanism other than transcriptional repression of these three cargo genes.

csrT represses *L. pneumophila* evasion of degradative lysosomes

Like hydrogen peroxide resistance, ICE-βox confers protection to *L. pneumophila* from degradative lysosomes in macrophage infection (97). Therefore, as an independent measure of *csrT* repression of ICE-βox-mediated resistance to oxidative stress, we quantified bacterial survival in macrophages, where *L. pneumophila* encounters oxidative radicals (81). Donor, transconjugant, and recipient strains ectopically expressing *csrT* were co-cultured with bone marrow derived mouse macrophages in the presence or absence of IPTG. After a 90 min infection, bacterial resistance to degradation was quantified by fluorescence microscopy. As expected, bacterial cells from uninduced ICE-positive donor and transconjugant cultures resisted degradation much like PE phase WT Lp02 cells (Figure 3.3C). However, when these same strains ectopically expressed *csrT*, the bacteria were more frequently degraded (~4-5 fold decrease in % intact bacteria, $P < 0.001$), as evident by particulate *L. pneumophila* antigen scattered throughout the macrophage, similar to E phase WT Lp02 cells (Figure 3.3C). In contrast, ICE-negative bacteria were not more frequently degraded after *csrT* induction. Therefore, similar to its effect on resistance to hydrogen peroxide, ectopic expression of *csrT* is sufficient to inhibit ICE-βox-conferred resistance to macrophage degradation, further supporting the model that CsrT is a repressor of ICE-βox-encoded traits.

To verify our microscopic assay of bacterial survival in macrophages (Figure 3.3C), we quantified cell-associated *L. pneumophila*. Bone marrow derived mouse macrophages were infected with donor, transconjugant and recipient strains carrying

pcsrT, and infectivity was quantified as the fraction of input bacteria that were viable and cell-associated after a 90 min macrophage infection. Ectopic expression of *csrT* markedly reduced infection efficiency in ICE-βox positive donor and transconjugant strains (Figure 3.3D, $P < 0.005$). In addition, induction of pcsrT also modestly decreased the already poor infectivity of the ICE-negative recipient strain (Figure 3.3D, $P < 0.001$). This observation suggested that, in addition to inhibiting ICE-βox-encoded traits, CsrT might also modulate components of the *L. pneumophila* core genome.

Induction of *csrT* inhibits *L. pneumophila* growth in macrophages

L. pneumophila containing ICE-βox replicate more efficiently in macrophages than those not containing the element (97). Because ectopic expression of *csrT* represses ICE-βox-mediated oxidative stress resistance in broth and in macrophages (Figure 3.3), we predicted *csrT* would also inhibit intracellular growth of *L. pneumophila*. To test the impact of *csrT* on intracellular replication, bone marrow-derived A/J mouse macrophages were infected with the donor strain cultured with or without IPTG to induce *csrT* expression. After 48 h, bacterial yield was quantified and expressed as fold increase relative to the number of intracelluar bacteria present at 2 h, to account for differences in infectivity (Figure 3.3D). As expected, the yield of intracellular bacteria was significantly reduced (~100 fold, $P < 0.005$) when *csrT* was ectopically expressed (Figure 3.4A).

Figure 3.4. CsrT inhibits replication in macrophages independent of NADPH oxidase

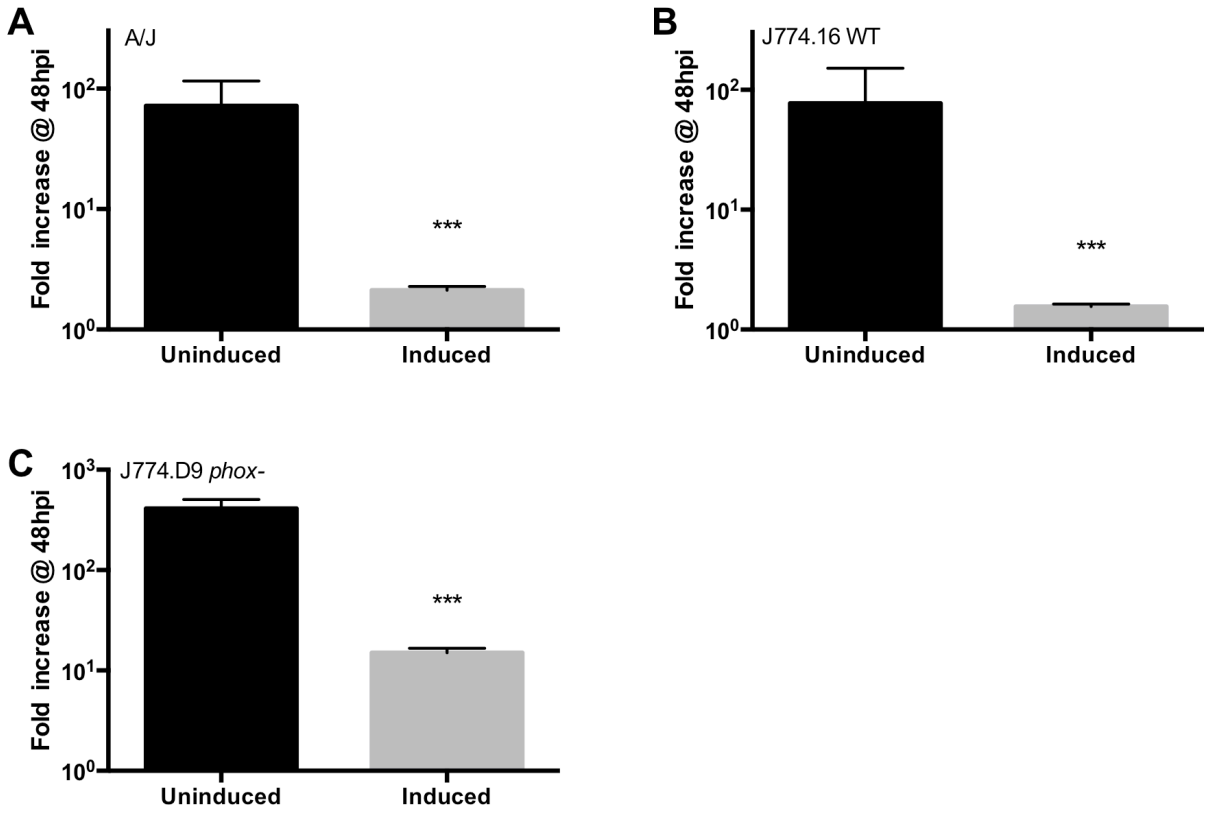

A), J774.16 WT macrophage cell line (B) and J774.D9 *phox* mutant macrophage cell line (C). Macrophages were infected with WT Lp02 carrying pcsrT (MB1383) treated +/- IPTG overnight prior to infection at an MOI of 1 (uninduced) or 2 (induced). Results are expressed as fold-increase of bacteria at 48 hours post infection (hpi) relative to the 2-hour timepoint (CFU 48hpi / CFU 2hpi) and shown are means +/- SEM from one experiment representative of three others. In all macrophage backgrounds, *T* tests confirm differences between uninduced and induced strains are significant ($P < 0.005$).

In macrophages, ICE-βox confers *L. pneumophila* protection to oxidative stress generated by the NADPH oxidase (97). To test whether the growth defect of strains induced to express *csrT* was due to the macrophage phagocyte oxidase, J774.16 WT and J774.D9 NADPH oxidase mutant macrophage cells were infected with the donor strain cultured with or without IPTG, and the yield of intracellular bacteria after 48 h was quantified. Much like the A/J mouse macrophage infection, the bacterial yield in J774.16 WT macrophages was significantly reduced by ectopic expression of *csrT* (~80-fold less, $P < 0.005$, Figure 3.4B). Moreover, *csrT* also reduced the yield of *L. pneumophila* in the J774.D9 NADPH oxidase mutants (~50 fold less, $P < 0.005$, Figure 4C). Therefore, ectopic expression of *csrT* inhibits *L. pneumophila* infection in macrophages by mechanism(s) that are not solely dependent on either the macrophage NADPH oxidase (Figure 3.4C) or ICE-βox (Figure 3.3D).

csrT inhibits motility and flagellar assembly in *L. pneumophila*

Efficient infection of macrophages by *L. pneumophila* requires not only evasion of the macrophage oxidative burst and phagosome-lysosome fusion (123, 134), but also motility, which increases bacterial contacts with host phagocytes (135). Our observation that ectopic expression of *csrT* decreased infectivity in a strain that lacks ICE-βox (Figure 3.3D) and replication in macrophages that lack NADPH oxidase (Figure 3.4C) suggests an effect of CsrT on the core *L. pneumophila* genome. Since motility is a broadly conserved trait encoded by the core genome that enhances infectivity, we investigated whether *csrT* expression represses motility. We were further motivated by the fact that canonical CsrA represses not only Dot/Icm T4SS activity but also motility

(110, 111, 136), indicating that *L. pneumophila* motility and T4SSs can belong to the same regulon. Indeed, when observed under a phase microscope, only ~ 5% of PE phase *L. pneumophila* that ectopically expressed *csrT*, were motile, as compared to approximately 90% of cells that were not induced to express *csrT* (Figure 3.5A).

To examine *csrT* inhibition of motility in more detail, we analyzed flagellin levels by western analysis of *L. pneumophila* cultured with and without *csrT* induction. As a positive control for flagellin repression, we induced ectopic expression of canonical *csrA*, which represses motility in *L. pneumophila* (110, 129). Similar to *csrA*, induction of *csrT* decreased flagellin protein levels (Figure 3.5A), indicating that both CsrA and CsrT inhibit flagellin production.

***csrT* inhibits motility in *B. subtilis* by a conserved RNA-binding mechanism**

As in *L. pneumophila*, the *B. subtilis* CsrA protein inhibits bacterial motility (121). Because the CsrA-binding site on its specific RNA target, *hag*, is defined in *B. subtilis*, we utilized this system to determine if CsrT can inhibit motility by the same molecular mechanism as the *B. subtilis* CsrA. In particular, we exploited a *B. subtilis* mutant, Δ*fliW sow3*, that is insensitive to CsrA repression of motility due to a point mutation in CsrA binding site on the *hag* mRNA and deletion of *fliW*, which encodes the protein that antagonizes CsrA (121). Swarming motility by *B. subtilis* wild-type and Δ*fliW sow3* mutant strains that ectopically expressed *L. pneumophila csrA* or *csrT* was quantified. Induction of either *csrA* or *csrT* each inhibited motility in wild-type *B. subtilis*, verifying

Figure 3.5. CsrT inhibits motility via a conserved mechanism.

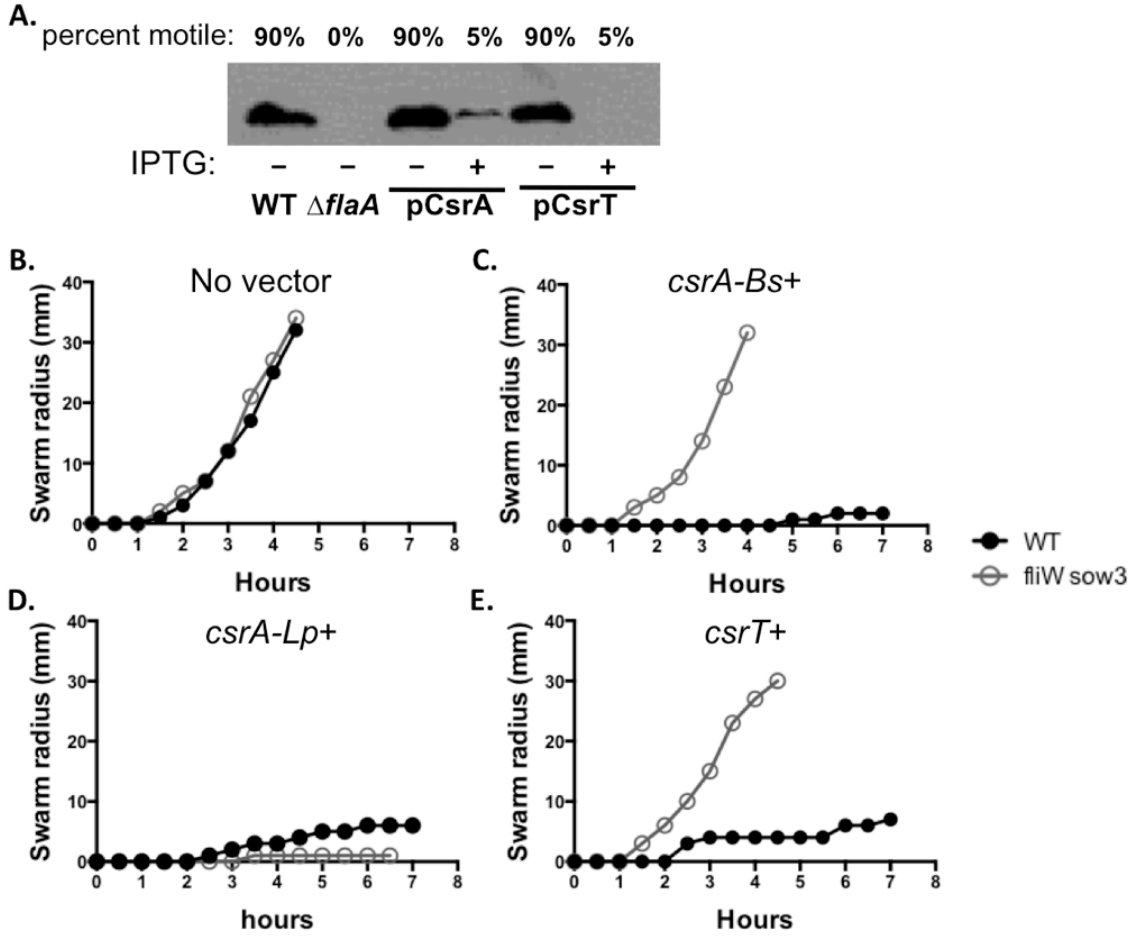

A) Western Blot for FlaA protein was performed on PE-phase cultures of Lp02 with pcsrA (MB1389) or pcsrT (MB1383), induced or not as indicated. Lp02 WT with no vector (MB110) was used as a positive control, and a *flaA* mutant (MB1390) as a negative control. Qualitative assessment of the percent motility of the cultures by inverted phase microscopy is indicated above. The blot is representative of at least 3 independent experiments.

B-E) Swarming motility was assessed every 30 minutes on swarm agar plates in *B. subtilis* WT (filled circles) and *fliW sow3* point mutants (open circles), which are insensitive to *B. subtilis* CsrA repression. Motility was assessed in WT (3610) and mutant (DS6530) with (B) no vector, (C) induced expression of *B. subtilis* CsrA (DS4940 and DK1469), (D) induced expression of *L. pneumophila* CsrA (DK675 and DK1470), and (E) induced expression of CsrT (DK677 and DK1471). Plots represent the means of triplicate plates from one experiment.

the assay is a sensitive readout of CsrA function. Neither *B. subtilis* CsrA nor *L. pneumophila* CsrT inhibited motility in the Δ*fliW sow3* mutant, which lacks the repressor's mRNA binding site. Since a single point mutation in the *hag* mRNA abrogated CsrT repression of motility, this CsrA paralog encoded by ICE-βox likely binds *hag* mRNA and represses its translation, consistent with a function as an RNA binding protein that recognizes the CsrA consensus sequence. In contrast, induction of canonical *L. pneumophila* CsrA inhibited *B. subtilis* swarming by a mechanism independent of the binding site defined for CsrA of *B. subtilis* (Figure 3.5D, E). Therefore, the CsrA encoded by the core *L. pneumophila* genome inhibits motility in *B. subtilis* by a different mechanism than the *B. subtilis* CsrA.

Discussion

Legionellae must adapt to assault from diverse environmental and intracellular stresses. Horizontally-acquired ICEs may increase the fitness of this opportunistic pathogen (62, 63, 66, 97, 113, 137). Here we demonstrate that every *L. pneumophila* ICE identified to date encodes a *csrA*-like locus that is genetically linked to a particular T4SS lineage. Further, our genetic analysis of *L. pneumophila* ICE-βox reveals that its *csrA* paralog *csrT* is a versatile regulator that cannot only repress the conjugative transfer and oxidative stress resistance encoded by the element, but also inhibit macrophage infection and bacterial motility when expressed ectopically.

By exploiting the well-characterized *B. subtilis* swarming motility pathway, we demonstrate that CsrT is likely an mRNA binding protein. Ectopic expression of *csrT* inhibited swarming motility in *B. subtilis* by a mechanism strictly dependent on the canonical CsrA binding site on the mRNA encoding flagellin (Figure 3.5D). Based on the observation that a point mutation of the *B. subtilis* CsrA binding site abrogated repression by ICE-βox *csrT*, we deduce that CsrT protein binds mRNA and specifically recognizes the ANGGA consensus sequence for CsrA binding that is used by several bacterial species (121, 138, 139). Indeed, the CsrT protein is endowed with many of the key residues that equip *E. coli* CsrA to bind mRNA (140)(Abbott 2015, in review). Together our genetic and bioinformatic data strongly suggest that, like canonical CsrA, CsrT is a post-transcriptional regulator. Future biochemical experiments can verify that CsrT protein directly interacts with mRNA targets and identify CsrT binding sites in *L. pneumophila*.

Our bioinformatic data suggest that an RNA target of CsrT may lie in its associated T4SS locus. Sequence alignment of 34 ICE-associated *csrA*-paralogs revealed at least four distinct gene families (Figure 3.1A). A combination of gene duplication events and subsequent genetic drift may have increased the size and diversity of this family of regulators. However, the high degree of similarity within each of the four distinct *csrA* groups may indicate that ICEs depend on their paralog to regulate specific pathways. The fact that each *csrA*-paralog cluster specifically correlates with one of four previously identified T4SS lineages – Lvh (129), Trb (69), Tra (97), and LGI (128) (Figure 3.1B) – predicts a functional relationship between ICE *csrA*

paralogs and T4SSs. Whereas the specific amino acid sequence of each *csrA* paralog appears to be genetically constrained by the composition of the adjacent T4SS locus, the same cannot be said for the associated cargo regions, which are diverse. Therefore, we favor the model that *csrA* paralogs regulate the core machinery of their T4SSs, rather than ICE cargo genes.

The prediction that ICE *csrA* paralogs regulate phenotypes conferred by their T4SSs is consistent with the capacity of canonical CsrA to regulate myriad *L. pneumophila* traits, including *dot/icm* T4SS protein substrate secretion (110, 111). Furthermore, CsrT repression of the ICE-βox T4SS would naturally extend from the hypothesis that CsrA is a regulator of nanomachinery, as was proposed in the *B. subtilis* system, where CsrA regulates flagellin (121). Indeed, we observed that ectopic expression of *csrT* reduced ICE-βox transfer ~ 10-fold (Figure 3.2). Consistent with regulation of the T4SS machinery by CsrT, we confirmed that the reduced conjugation could not be accounted for by a defect in ICE-βox excision (data not shown), unlike the impact of the *csrA* locus encoded by the Trb-1 ICE (70). In addition, although ectopic expression of *csrT* inhibited ICE-βox-mediated resistance to hydrogen peroxide (Fig 3.3A), this repression was not due to reduced transcript levels of putative effectors in the cargo region (Figure 3.3B). Therefore our phenotypic and bioinformatic data and knowledge of regulation by canonical CsrA (129) are consistent with the model that CsrT regulates its T4SS machinery.

In addition to repression of the ICE-βox-mediated phenotypes (Figure 3.3A, C), *csrT* also inhibited macrophage infection in part by a mechanism(s) independent of ICE-

βox. When expressed ectopically, *csrT* reduced the infectivity and intracellular yield of *L. pneumophila* whether or not the strain carried ICE-βox (Figure 3.3D, data not shown). Furthermore, *csrT* reduced the bacterial yield in the J774.D9 phagocyte oxidase mutant cell line that is permissive for growth of *L. pneumophila* that do or do not encode ICE-βox (97) (Figure 3.4C). The observation that ectopic expression of *csrT* repressed macrophage infections independently of ICE-βox suggests that CsrT may regulate components of the core genome.

Indeed, CsrT inhibits flagellin expression and motility (Figure 3.5A), a broadly conserved trait that contributes to *L. pneumophila* virulence (110). Reduced motility likely contributes to CsrT's inhibition of infectivity (Figure 3.3D, 3.5A) – amotile *L. pneumophila* are less infectious in cell culture due to decreased contacts with macrophages (135). CsrT repression of motility may increase ICE-βox fitness because a stationary host conjugates more efficiently; alternatively, its inhibition of flagellin production may simply reflect its ancestry as a homologue of canonical CsrA, a repressor of *L. pneumophila* motility (110). On the other hand, ectopic expression of two other ICE-associated *csrA*-paralogs was not sufficient to inhibit *L. pneumophila* motility (*lpg1257* and *lpg1003*, data not shown). Accordingly, we speculate that genetic drift of individual ICE *csrA* paralogs may accommodate distinct regulatory demands of their corresponding T4SS class (Figure 1), concomitantly relaxing their capacity to repress motility.

The observation that ectopic expression of *csrT* inhibits phenotypes as diverse as ICE-βox conjugation and host motility provides insight to why *csrA* regulators are

ubiquitous among *L. pneumophila* ICEs. CsrA is a pluripotent post-transcriptional repressor of transmission traits that *L. pneumophila* requires for replication *in vitro* and in macrophages and amoebae (110). It follows that the capacity of a *csrA* paralog to manipulate a core life-cycle switch of its host bacterium would increase the fitness of these horizontally-acquired conjugal elements. A post-transcriptional regulator would equip the ICE to load its host cell with a pool of transcripts whose translation can be quickly de-repressed when environmental conditions favor ICE spread.

CHAPTER FOUR

Discussion

Legionella pneumophila has the remarkable ability to survive in a wide range of intracellular and extracellular environments. The diversity and abundance of niches for the bacteria makes it particularly hard to eradicate. The pathogen can replicate within evolutionarily distant amoebae and alveolar macrophages or form cyst-like environmental forms suitable for persistence and survival in stringent conditions. In the absence of a host, planktonic *Legionella* can create or join existing biofilms on natural and man-made surfaces, protecting itself from environmental insult.

Some of this lifestyle versatility can be attributed to the mosaic *L. pneumophila* genome. *L. pneumophila* are naturally competent and contain recombination machinery that facilitates genome remodeling, including acquisition of new genetic material from other species. The bacteria carry many eukaryotic-like proteins, likely acquired horizontally from amoebae hosts, that enhance persistence and reorganization of cell components during infection (63, 65). An additional source of genomic variability is the accessory genome. *Legionella spp.* draw from a pool of mobile genetic elements such as transposons and conjugative plasmids to acquire new traits not necessary for infection. These accessory traits increase *Legionella* diversity and persistence in low temperature and oxidative environments (97, 141).

Based on evidence that mobile genetic elements provide *L. pneumophila* with specific survival advantages (97, 141), I probed the function of the 65-kb LpPI-1 region, renamed ICE-βox, that is carried in 18% of 217 isolates surveyed (65). In Chapter Two, I confirmed that ICE-βox is a conjugative element and demonstrated its contribution to *L. pneumophila* oxidative stress resistance *in vitro* and in macrophages. Having established that ICE-βox protects *L. pneumophila* from the macrophage phagocyte oxidase (97), the next goal was to elucidate the specific ICE-βox factors and mechanisms responsible for this resistance.

Of the 38 predicted cargo genes carried on ICE-βox, several resemble oxidative stress response genes. Using BLAST alignment and Phyre2 structural modeling of each ORF, I identified a number of cargo genes of particular interest. For instance, multiple copies of the methionine sulfoxide reductase genes *msrA* and *msrB* are carried as ICE-βox cargo. As discussed in Chapter Two, these stereo-specific enzymes act to reduce oxidized methionine residues on damaged proteins and facilitate protein refolding (87). Across bacterial species, *msrAB*s are critical for detoxification after oxidative damage with hydrogen peroxide or during macrophage infection (86-88). *L. pneumophila* encodes one *msrA* copy on its core chromosome; thus, the three additional copies on ICE-βox may increase the level or timing of protection from oxidative stress.

Divergently encoded from one *msrB* locus is the lifecycle marker *magA*. MagA has been characterized as a marker of the Mature Intracellular Form (MIF) of *L. pneumophila (142).* MIFs are infectious, cyst-like *L. pneumophila* forms distinct from stationary phase bacteria that are predicted to enhance versatility in the environment

(142). MIFs contain 10-fold higher levels of MagA protein during morphogenesis of MIFs generated within cultured HeLa cells (143). However, *magA* is not essential for the development of this *L. pneumophila* life form since its deletion does not abrogate MIF formation (143). At the structural level, this gene is a homolog of alkyl hydroperoxide reductases (*ahpD). Ahp* proteins are important for scavenging peroxide radicals during intracellular infection and exposure to hydrogen peroxide *in vitro* (89), the precise conditions in which ICE-βox is beneficial. Its homology to *ahpD* enzymes could implicate *magA* in redox cycling after exposure to oxidative stress encountered as a MIF. Like *msrAB,* an *ahpD* homolog is also encoded on the core *L. pneumophila* chromosome. It remains to be determined if ICE-βox confers advantages to MIF formation or survival.

A final putative oxidative responsive cargo gene of interest identified by sequence analysis is an ortholog of the bacterial cytochrome c subunit III (*lpg2100*), a terminal electron acceptor during bacterial respiration. While the mechanism has not been well studied, cytochrome c proteins have been implicated in oxidative stress resistance in response to hydrogen peroxide (144). Like cytochrome C oxidase, *msrAB* and *ahpD* are membrane-bound proteins that are poised to act as soon as reactive oxygen species are encountered. Of the predicted cargo genes, these three were postulated to be the strongest contributors to the oxidative stress resistance phenotype conferred by ICE-βox (97).

A few pilot studies of the effects of these cargo genes on stress resistance were performed. To test if the *msrAB* operon was sufficient to provide resistance, the locus was cloned into an inducible expression vector and transformed into ICE-βox-negative

recipient strains. However, *msrAB*-induced strains were not more resistant than uninduced strains in the presence of hydrogen peroxide or in macrophages, even though their increased production was confirmed after separating the protein pool by gel electrophoresis. Other ICE-βox-encoded factors are likely necessary to coordinate the response to these stressors. I also applied a loss-of-function approach by creating a *magA* deletion in the ICE-βox donor strain. Similar to the *msrAB* overexpression results, *magA* mutants survived as well as wild type in *in vitro* and *in vivo* oxidative conditions. This is perhaps not surprising, as bacteria typically encode many layers of redundant detoxification systems; therefore, deletion of one should not make cells more vulnerable. Finally, the transcriptional response of *msrA*, *magA* and *lpg2100* to oxidative stress was probed using RNA isolated from ICE-βox cultures treated or not with hydrogen peroxide. Interestingly, while *lpg2100* RNA levels increased in response to this stressor, *msrA* and *magA* transcript levels were significantly lower as compared to untreated cultures. Together these preliminary results did not identify a single ICE-βox cargo gene that accounts for the oxidative stress resistance in strains that harbor the ICE. I favor the model that multiple cargo genes work in concert and that their expression is tightly regulated to respond to specific conditions. Indeed, also encoded as cargo are homologs of efflux pumps (*lpg2109*) and ABC transporters (*lpg2063-lpg2064).* These pumps contribute to the resistance of β-lactam antibiotics in *E. coli* and *P. aeruginosa* by creating a pore for the extrusion of antibiotic compounds (145, 146). A combination of detoxifying enzymes and efflux pumps could rescue the bacteria from reactive oxygen byproducts and reduce the amount of antibiotic that enters the cell. To

test these models, a more rigorous molecular genetic analysis is necessary to determine the mechanism of ICE-βox protection.

Approximately 40% of ICE-βox cargo genes are annotated as hypothetical proteins that do not have homology to any known genes. These putative proteins contain Domains of Unknown Function that, while often highly conserved among bacterial genera, are yet to be characterized. It is possible that the genes responsible for ICE-βox traits are among this class of cargo loci. A few other cargo genes are predicted to contribute to oxidative stress resistance based on homology to known proteins. One is a glutathione S-transferase (GST, *lpg2104*), an enzyme critical for conjugation of glutathione to detoxify reactive oxygen substrates. This enzyme could work in concert with the ICE-encoded cytochrome C subunit (*lpg2100*). In one potential model, stressed bacteria would first activate cytochrome C to increase ATP levels. This signal, in turn, would drive the production of glutathione and subsequently detoxify the cell using the encoded GST. Like *msrAB, magA* and *lpg2100*, *L. pneumophila* encodes additional GSTs on its core chromosome as well as on ICE-βox. It could be that the oxidative stress resistance effect conferred by ICE-βox is mediated by additional copies of antioxidant proteins such as these. Alternatively, these cargo genes may respond to distinct signals to offer protection in conditions in which the core enzymes are not expressed.

To examine more rigorously the contribution of individual cargo genes to ICE-βox traits, I propose that future studies apply unbiased screening approaches. First, transposon mutagenesis of the cargo regions would generate a pool of mutants in

ORFs of interest as well as genes of unknown function. Screening for loss of oxidative stress resistance could identify genes critical for this response. Similarly, a gain-of-function approach could be applied by creating expression vectors containing overlapping fragments of cargo region DNA. Transformation of an ICE-βox-negative recipient strain with this cargo vector pool and subsequent exposure to oxidants would reveal if specific cargo or operons are sufficient to provide protection to a naïve host. Finally, a complimentary approach would be directed mutagenesis of genes or full operons of interest. However, given the size of the cargo regions (~40 kb) a screening approach is likely to be more efficient. Importantly, these approaches should be conducted on genomic DNA isolated specifically from the ICE cargo regions so to avoid disrupting critical regulatory or structural genes on the element. A better understanding of the mechanism of ICE-βox oxidative stress resistance will further our understanding of how *L. pneumophila* uses accessory genes to adapt to stringent environments.

ICE-βox Regulation

ICEs encode both T4SS machinery and cargo enzymes and expression of each component is likely carefully regulated. In Chapter Three, we identify four distinct families of T4SS represented among *Legionella* ICEs. There are also a series of conserved regulatory genes immediately preceding each T4SS transfer apparatus (Figure 3.1B). The regulatory region of each T4SS locus contains a distinct paralog of the master regulator *csrA*, which is co-inherited with a specific class of T4SS. ICE-βox specifically carries the *csrA* paralog, *csrT*, in this region. CsrT represses some of the

oxidative stress resistance provided by ICE-βox (Figure 3.3). CsrT does not appear to be sufficient to repress all ICE-βox traits, however, as its ectopic expression in rich medium had only a moderate inhibitory effect on transfer of the element (Figure 3.2). Given its similarity to canonical *csrA* of *L. pneumophila* and capacity to substitute for *B. subtiliis csrA*, CsrT may function as a post-transcriptional regulator in a complex regulatory cascade.

Also co-inherited with the 5' ICE-βox region are three other putative regulatory genes. These genes, *lvrRAB*, immediately precede the *csrA* paralog (also known as *lvrC*). Two of these genes (*lvrAB)* appear to be transcribed with *csrT* from one operon, while the *lvrR* is divergently expressed. BLAST analysis of *lvrAB* does not reveal similarity to characterized proteins but does reveal high homology to genes in various *Legionella* ICEs. Phyre2 predicted protein structures reveal weak structural similarity to phage DNA-binding replisome proteins, consistent with the likely ancestry of these mobile elements.

The *lvrR* gene, however, is a homolog of the transcriptional prophage cI repressor that is similar to LexA. As part of the bacterial SOS response, LexA binds to SOS response gene promoters and blocks transcription in response to DNA damaging agents (147). LexA represses polymerase genes necessary for DNA repair. But once bound by the master regulator RecA, LexA cleaves itself, derepressing transcription. This conserved regulatory mechanism is useful for regulation of ICE traits, as many ICE cargo genes often mitigate the effects of xenobiotics and can also protect the host cell

(3). Conservation of a LexA repressor may equip the ICE to respond rapidly to stressful conditions sensed by the host bacterium.

Activation of the SOS response can induce horizontal gene transfer of mobile elements, including ICEs (148). In the event of chemical stress, the SOS response would allow ICEs to escape a damaged bacterial cell and enter a new host (149). Indeed, ICE-SXT from *Vibrio cholerae* transfers in response to antibiotics (16). The element encodes a LexA-like regulator SetR that is cleaved upon antibiotic exposure, allowing transcription of the T4SS conjugation apparatus and integrase enzymes necessary for mobilization (16). Similarly, the DNA damaging agent mitomycin C activates ICE*Bs1* excision and transfer in *Bacillus subtilis* by inducing the SOS response and relief of ImmR repression of ICE genes (6, 149, 150). Carrying SOS-responsive regulatory elements may provide ICEs additional advantages after conjugation into a new host, as there is evidence that incoming ICE DNA triggers this conserved response pathway, which promotes efficient recombination and integration into the chromosome (151). Importantly, the SOS-responsive ICEs do not carry their own copy of the RecA activating gene and thus must rely on the host enzyme to sense stress and trigger LexA proteolysis. By integrating their regulatory systems with host cascades, ICEs exploit this conserved mechanism to sense and respond to host bacterium stress.

There is evidence that the LexA-like *lvrR* genes conserved in *Legionella* ICEs function similarly to those described in other systems. Indeed, the *lvrR* regulator carried on ICE Trb-1 from *L. pneumophila* Corby acts as a repressor of excision (70). The effect of *lvrR* on cargo traits was not examined in this study, as a phenotypic advantage of ICE

Trb-1 has not been identified. Although LexA-like genes are conserved on ICEs, *Legionella* lacks a core chromosomal copy of the canonical LexA (152). This characteristic is not unusual; many pathogens also lack this regulator (153). However unlike other pathogens, the SOS response in *Legionella* appears to be atypical, as RecA does not respond to UV- or mitomycin C-induced damage (152, 154). Accordingly, it is not clear if this atypical response would affect the ICE-encoded LexA-like repressor *lvrR* in the same manner as in other systems.

In Chapter Three, we reported that ectopic expression of *csrT* inhibits transfer and oxidative stress resistance provided by ICE-βox (Figure 3.2, 3.3), consistent with a repressor. However, a cursory examination of transcription levels of putative oxidative-responsive cargo genes showed that ectopic expression of *csrT* leads to induction of some cargo genes, not repression (Fig 3.3). As oxidative stress is a prime activator of the prototypical SOS response, induction of these genes could be under regulatory control of a DNA binding protein like *lvrR.* In this case, we would predict that ectopic expression of *lvrR* in oxidative conditions would repress cargo gene transcription and even more dramatically alter the oxidative stress response.

I favor the model that *csrT* is an mRNA binding protein like *csrA.* The canonical *csrA* functions as a post-transcriptional regulator by binding to the Shine-Dalgarno sequence of transmissive phase mRNA traits in *L. pneumophila* (51, 111). Upon sensing nutrient limitation, a complex signaling cascade induces the production of the small non-coding RNAs (ncRNA) RsmY and RsmZ. These bind and sequester CsrA from the target mRNA, derepressing translation (155). ICE-βox *csrT* may use a similar

mechanism to regulate expression of cargo or transfer genes. Indeed, deep sequencing of *L. pneumophila* during infection revealed three putative encoded ncRNAs located in the ICE-βox cargo regions, ncRNAs (lpr0046-48) (156). Independent studies showed that the ncRNA lpr0035, encoded on ICE-lvh, increases *L. pneumophila* entry into macrophages and amoebae by a pathway that depends on ICE-lvh cargo genes (157). Although a mechanism of regulation was not identified, it is possible that, like RsmYZ, ICE-encoded ncRNAs are activated in ICE-inducing conditions to relieve post-transcriptional repression by *csrA* paralogs.

To elucidate whether components of the SOS response or small RNAs contribute to ICE-βox activation, classic genetic tools can be applied. By creating directed mutants in *lvrR* and the ncRNAs, one can determine if loss of these putative regulators affects oxidative stress resistance or transcription of ICE-βox cargo genes. Using ectopic expression plasmids, the putative inhibitory effect of *lvrR* on ICE mobilization and transfer can be examined. By creating expression plasmids that contain both the ncRNA and *csrT*, one could test whether ncRNAs can directly relieve repression by *csrT* in a manner similar to the CsrA-RsmYZ interaction. Preliminary evidence suggests a link between these two components. Quantitative PCR examining transcription of ICE-βox ncRNAs in cultures that ectopically express *csrT* determined that levels of all three ncRNA are higher in cells expressing *csrT* compared to uninduced controls (data not shown). Based on genetic and bioinformatic evidence that ICE-βox is equipped with two distinct regulatory mechanisms, I speculate that each system may control a distinct regulon, either the oxidative-responsive genes or transfer machinery. A better

understanding of this putative regulatory cascade will clarify the selective pressures on *Legionella* ICEs for co-inheritance of these regulatory regions with T4SS loci.

ICE-βox Epidemiology

Since ICE-βox enhances *L. pneumophila* resistance to oxidative stresses encountered *in vitro* and *in vivo*, its spread by horizontal gene transfer poses potential risks to human health. To assess the prevalence of integrated ICE-βox or the *att* site necessary to acquire the element in three categories of *L. pneumophila* isolates, we designed a multiplex PCR screen. First, to see if presence of ICE-βox correlates with clinical activity, we will examine the element's prevalence in *L. pneumophila* outbreak isolates. To test the hypothesis that use of chlorine-based disinfectants selects for the proliferation of *L. pneumophila* carrying ICE-βox, we will screen isolates obtained from built environments with known disinfection protocols. We will compare these ICE-βox frequencies to those of isolates obtained from natural water with no known exposure to biocides. By obtaining a comprehensive picture of ICE-βox prevalence in different *L. pneumophila* niches, we can assess the potential for enrichment and spread of these mobile elements that increase *L. pneumophila* fitness and virulence.

For this study, we are collaborating with the Centers for Disease Control *Legionella* laboratory. However, because the CDC mainly receives *L. pneumophila* samples from outbreaks, their pilot study did not contain sufficient numbers of samples from each of the isolate categories we intend to screen. In particular, their collection primarily contains isolates of the pathogenic serogroup 1 and does not represent a

diverse collection of *L. pneumophila*. Nevertheless, the preliminary results from this screen are still informative.

To date, our collaborators at the CDC have screened 183 clinical and environmental isolates. Of all isolates tested, 57 (31.1%) contained integrated ICE-βox, and the remaining 126 (68.9%) carry the *att* site (Table 4.1). Of the 183 isolates, 113 were serogroup 1 strains; within this subset, 24/84 (28.5%) of clinical samples and 22/29 (75.8%) of built environment isolates carried ICE-βox (Table 4.1). While there are only limited data on the water treatment protocols used in these built environment sources, data from three outbreak locations where ICE-βox strains were isolated show use of chlorine disinfectants at concentrations ranging from 0.2-0.7 ppm Cl_2. Only one isolate was tested from natural water in Thailand, and ICE-βox was not detected in this strain. Of non-serogroup 1 strains, the prevalence of integrated ICE-βox was overall much lower in both clinical (8.2%) and environmental (29.4%) isolates compared to serogroup 1 strains (Table 4.1).

Our preliminary results from this epidemiological screen verify the multiplex PCR assay is robust and can detect ICE-βox in a range of *L. pneumophila* serotypes. It is interesting that among all strains tested, ICE-βox is more often found in built environment isolates than clinical samples. Though we have shown experimentally that ICE-βox offers *L. pneumophila* advantages in mouse macrophage cultures, it appears that the element is even more beneficial in the environment (eg, 28.5% clinical vs 75.8% environment). This apparent enrichment of ICE-βox in environmental strains is consistent with the hypothesis that disinfectant-treated water selects for ICE-βox

containing strains. However, these populations must be screened much more thoroughly before we can draw a link between specific treatment regimens and ICE-βox prevalence. Similarly, it is tempting to speculate that ICE-βox contributes to pathogenicity as it is found more frequently in serogroup 1 strains than other serogroups. Again, a more rigorous screen is needed, and an analysis of the impact of LPS structure on ICE-βox conjugation is warranted. With these caveats in mind, we are eager to probe a much larger set of natural *L. pneumophila* isolates with no known exposure to biocides to determine the prevalence of ICE-βox in *L. pneumophila* within natural waters.

All 183 isolates tested contained the *att* site, indicating these bacteria have the capacity to integrate ICE-βox should it be acquired in the environment. Importantly, the *att* site appears to be species-specific, as it was not found when other microorganisms were screened by BLAST search. Thus, while ICE-βox remains a threat to the evolution of more resistant *L. pneumophila* strains, its spread to other species does not appear likely. Continued analyses of a larger natural and environmental isolate collection for both ICE-βox and its integration site will be highly informative for public health and safe water treatment practices.

Conclusion

L. pneumophila remains an accidental pathogen of human alveolar macrophages. The bacteria have evolved over time to persist in the environment and only cause disease in humans after aerosolization of contaminated water. The

extracellular environment and intracellular vacuoles in amoebae and macrophages can contain stringent chemicals and thus *L. pneumophila* has evolved mechanisms to tolerate harsh stressors such as oxidants. Indeed, acquisition of integrative conjugative elements such as ICE-βox provides *L. pneumophila* the ability to detoxify oxidative stressors such as bleach. Human activities promote the evolution of resistant organisms. Much like overuse of antibiotics on factory farms has selected for multiply antibiotic resistant pathogens, overuse of chlorine-based disinfectants may increase the burden of resilient *L. pneumophila* by contributing to the spread of resistance determinants such as ICE-βox. With continued research, we can develop more effective disinfection protocols to eradicate resistant *L. pneumophila* from built environments and to reduce the occurrence of death and disease in humans.

Table 4.1 ICE-βox prevalence in *L. pneumophila* isolates from the CDC

Isolate Source	**Contains ICE-βox**	**Contains *att* site**	**Location examples**
Clinical	24/84 (28.6%)	60/84 (71.4%)	Lung, sputum, bronchial wash
Built environment	22/29 (75.8%)	7/29 (24.1%)	Cooling tower, faucet, fountain
Cl_2 exposure	2/3 (66.6%)	1/3 (33.3%)	Source treated with 0.2-0.7ppm Cl_2
Natural environment	0/1 (0%)	1/1 (100%)	Soil and outdoor shower in Thailand
Non Sg1 Clinical	4/49 (8.2%)	45/49 (91.8%)	Lung, sputum, bronchial wash
Non Sg 1 Environmental	5/17 (29.4%)	12/17 (70.6%)	Faucet, showerhead, tap water

Multiplex PCR for integrated ICE-βox (second column) or the *att* site (third column) on DNA isolated from *L. pneumophila* outbreak isolates. The first four rows represent screening results from serogroup 1 strains; the last two rows cover non-serogroup 1 strains.

BIBLIOGRAPHY

1. Cascales E & Christie PJ (2003) The versatile bacterial type IV secretion systems. *Nat Rev Microbiol* 1(2):137-149.

2. Juhas M, Crook DW, & Hood DW (2008) Type IV secretion systems: tools of bacterial horizontal gene transfer and virulence. *Cell Microbiol* 10(12):2377-2386.

3. Wozniak RA & Waldor MK (2010) Integrative and conjugative elements: mosaic mobile genetic elements enabling dynamic lateral gene flow. *Nat Rev Microbiol* 8(8):552-563.

4. Juhas M (2015) Horizontal gene transfer in human pathogens. *Crit Rev Microbiol* 41(1):101-108.

5. Brown-Jaque M, Calero-Caceres W, & Muniesa M (2015) Transfer of antibiotic-resistance genes via phage-related mobile elements. *Plasmid* 79:1-7.

6. Auchtung JM, Lee CA, Garrison KL, & Grossman AD (2007) Identification and characterization of the immunity repressor (ImmR) that controls the mobile genetic element ICEBs1 of Bacillus subtilis. *Mol Microbiol* 64(6):1515-1528.

7. Osborn MA, Boltner, D. (2002) When phage, plasmids, and transposons collide: genomic islands, and conjugative- and mobilizable-transposons as a mosaic continuum. *Plasmid* 48(3):10.

8. Gyles C & Boerlin P (2014) Horizontally transferred genetic elements and their role in pathogenesis of bacterial disease. *Vet Pathol* 51(2):328-340.

9. Boltner D, MacMahon C, Pembroke JT, Strike P, & Osborn AM (2002) R391: a Conjugative Integrating Mosaic Comprised of Phage, Plasmid, and Transposon Elements. *J Bacteriol* 184(18):5158-5169.

10. Sobecky PA & Coombs JM (2009) Horizontal Gene Transfer in Metal and Radionuclide Contaminated Soils. *Meth Mol Biol* 532.

11. Baker-Austin C, Wright MS, Stepanauskas R, & McArthur JV (2006) Co-selection of antibiotic and metal resistance. *Trends Microbiol* 14(4):176-182.

12. Nies DH (2003) Efflux-mediated heavy metal resistance in prokaryotes. *FEMS Microbiol Rev* 27(2-3):313-339.

13. Mikkelsen H, Hui K, Barraud N, & Filloux A (2013) The pathogenicity island encoded PvrSR/RcsCB regulatory network controls biofilm formation and dispersal in Pseudomonas aeruginosa PA14. *Mol Microbiol* 89(3):450-463.

14. Giedraitiene A, Vitkauskiene A, Naginiene R, & Pavilonis A (2011) Antibiotic Resistance Mechanisms of Clinically Important Bacteria. *Medicina (Kaunas)* 47(3):137.

15. Wright GD (2007) The antibiotic resistome: the nexus of chemical and genetic diversity. *Nat Rev Microbiol* 5(3):175-186.

16. Beaber JW, Hochhut B, & Waldor MK (2004) SOS response promotes horizontal dissemination of antibiotic resistant genes. *Nature* 427:72-74.

17. Sentchilo V*, et al.* (2009) Intracellular excision and reintegration dynamics of the ICEclc genomic island of Pseudomonas knackmussii sp. strain B13. *Mol Microbiol* 72(5):1293-1306.

18. Wang Y, Shoemaker NB, & Salyers AA (2004) Regulation of a Bacteroides Operon That Controls Excision and Transfer of the Conjugative Transposon CTnDOT. *J Bacteriol* 186(9):2548-2557.

19. Bose B, Auchtung JM, Lee CA, & Grossman AD (2008) A conserved anti-repressor controls horizontal gene transfer by proteolysis. *Mol Microbiol* 70(3):570-582.

20. Allen HK*, et al.* (2010) Call of the wild: antibiotic resistance genes in natural environments. *Nat Rev Microbiol* 8(4):251-259.

21. Segura PA, Francois M, Gagnon C, & Sauve S (2009) Review of the occurrence of anti-infectives in contaminated wastewaters and natural and drinking waters. *Environ Health Persp* 117(5):675-684.

22. Thiele-Bruhn S (2003) Pharmaceutical antibiotic compounds in soils - a review. *J. Plant Nutr. Soil Sci.* 166.

23. Rhodes G, Huys, G., Swings, J., Mcgann, P., Hiney, M., Smith, P., Pickup, R. W. (2000) Distribution of oxytetracycline resistance plasmids between Aeromonads in hospital and aquaculture environments: Implication of Tn1721 in Dissemination of the Tetracycline resistance determinant TetA. *Appl Env Microbiol* 66(9).

24. Sarmah AK, Meyer MT, & Boxall AB (2006) A global perspective on the use, sales, exposure pathways, occurrence, fate and effects of veterinary antibiotics (VAs) in the environment. *Chemosphere* 65(5):725-759.

25. Ward MJ*, et al.* (2014) Time-scaled evolutionary analysis of the transmission and antibiotic resistance dynamics of Staphylococcus aureus CC398. *Appl Env Microbiol*

26. Fraser DW, Tsai, T. R., Orenstein, W., Parkin, W. E., Beecham, H. J., Sharrar, R. G., Harris, J., Mallison, G. F., Martin, S. M., McDade, J. E., Shepard, C. C., Brachman, P. S. (1977) Legionnaires' Disease - Description of an Epidemic of Pneumoni. *N Engl J Med* 297.

27. Katz SM (1978) The morphology of the Legionnaires' disease organism. *Am J Pathol.* 90(3).

28. Phin N*, et al.* (2014) Epidemiology and clinical management of Legionnaires' disease. *Lancet Infect Dis* 14(10):1011-1021.

29. Marston BJ, Lipman, H. B., Breiman, R. F. (1994) Surveillance for Legionnaires' Disease. *Arch Intern Med* 154(21).

30. Abdel-Nour M, Duncan C, Low DE, & Guyard C (2013) Biofilms: the stronghold of Legionella pneumophila. *Int J Mol Sci* 14(11):21660-21675.

31. Yu PY*, et al.* (2008) The high prevalence of Legionella pneumophila contamination in hospital potable water systems in Taiwan: implications for hospital infection control in Asia. *International journal of infectious diseases : Int J Infect Dis* 12(4):416-420.

32. Fields BS (1996) The molecular ecology of legionellae. *Trends Microbiol* 4(7).

33. van Heijnsbergen E*, et al.* (2015) Confirmed and Potential Sources of Legionella Reviewed. *Env Sci Technol*.

34. Molmeret M, Horn, M., Wagner, M., Santic, M., Kwaik, Y. A. (2005) Amoebae as training grounds for intracellular bacterial pathogens. *Appl Env Microbiol* 71(1):8.

35. Bruggemann H*, et al.* (2006) Virulence strategies for infecting phagocytes deduced from the in vivo transcriptional program of Legionella pneumophila. *Cell Microbiol* 8(8):1228-1240.

36. Hammer BK, Tateda ES, & Swanson MS (2002) A two-component regulator induces the transmission phenotype of stationary-phase Legionella pneumophila. *Mol Microbiol* 44(1):107-118.

37. Barker J, Brown, M. R., Collier, P. J., Farrell, I., Gilbert, P. (1992) Relationship between Legionella pneumophila and Acanthamoeba polyphaga: physiological status and susceptibility to chemical inactivation. *Appl Env Microbiol* 58(8).

38. Kwaik YA, Gao, L.Y., Stone, B. J., Venkataraman, C., Harb, O. S. (1998) Invasion of Protozoa by *Legionella pneumophila* and Its Role in Bacterial Ecology and Pathogenesis. *Appl Env Microbiol* 64(9).

39. Cirillo JD, Falkow, S., Tompkins, L. S. (1994) Growth of *Legionella pneumophila* in *Acanthamoeba castellanii* enhances invasion. *Infect Immun 62* (8).

40. Richards AM, Von Dwingelo JE, Price CT, & Abu Kwaik Y (2013) Cellular microbiology and molecular ecology of Legionella-amoeba interaction. *Virulence* 4(4):307-314.

41. Berk SG, Ting, R. S., Turner, G. W., Ashburn, R. J. (1998) Production of respirable vesicles containing live *Legionella pneumophila* Cells by Two *Acanthamoeba* spp. *Appl Env Microbiol* 64(1).

42. Bigot R, Bertaux J, Frere J, & Berjeaud JM (2013) Intra-amoeba multiplication induces chemotaxis and biofilm colonization and formation for Legionella. *PloS One* 8(10):e77875.

43. Emtiazi F, Schwartz T, Marten SM, Krolla-Sidenstein P, & Obst U (2004) Investigation of natural biofilms formed during the production of drinking water from surface water embankment filtration. *Water Res* 38(5):1197-1206.

44. Merault N*, et al.* (2011) Specific real-time PCR for simultaneous detection and identification of Legionella pneumophila serogroup 1 in water and clinical samples. *Appl Env Microbiol* 77(5):1708-1717.

45. Chiao TH, Clancy TM, Pinto A, Xi C, & Raskin L (2014) Differential resistance of drinking water bacterial populations to monochloramine disinfection. *Environ Sci Technol* 48(7):4038-4047.

46. Roy CR, Berger KH, & Isberg RR (1998) Legionella pneumophila DotA protein is required for early phagosome trafficking decisions that occur within minutes of bacterial uptake. *Mol Microbiol* 28(3):663-674.

47. Swanson MS & Isberg RR (1996) Analysis of the Intracellular Fate of *Legionella pneumophila* Mutants. *Annals N. Y. Acad Sci* 797:8-18.

48. Molofsky AB & Swanson MS (2004) Differentiate to thrive: lessons from the Legionella pneumophila life cycle. *Mol Microbiol* 53(1):29-40.

49. Dalebroux ZD, Edwards RL, & Swanson MS (2009) SpoT governs Legionella pneumophila differentiation in host macrophages. *Mol Microbiol* 71(3):640-658.

50. Dalebroux ZD, Yagi BF, Sahr T, Buchrieser C, & Swanson MS (2010) Distinct roles of ppGpp and DksA in Legionella pneumophila differentiation. *Mol Microbiol* 76(1):200-219.

51. Molofsky AB & Swanson MS (2003) Legionella pneumophila CsrA is a pivotal repressor of transmission traits and activator of replication. *Mol Microbiol* 50(2):445-461.

52. Sauer JD, Bachman MA, & Swanson MS (2005) The phagosomal transporter A couples threonine acquisition to differentiation and replication of Legionella pneumophila in macrophages. *Proc Nat Acad Sci U. S. A.* 102(28):9924-9929.

53. Byrne B & Swanson MS (1998) Expression of *Legionella pneumophila* Virulence Traits in Response to Growth Conditions. *Infect Immun* 66(7):3029-3034.

54. Byrne BG, Dubuisson JF, Joshi AD, Persson JJ, & Swanson MS (2013) Inflammasome components coordinate autophagy and pyroptosis as macrophage responses to infection. *mBio* 4(1):e00620-00612.

55. Molofsky AB*, et al.* (2006) Cytosolic recognition of flagellin by mouse macrophages restricts Legionella pneumophila infection. *J Exp Med* 203(4):1093-1104.

56. Lightfield KL*, et al.* (2008) Critical function for Naip5 in inflammasome activation by a conserved carboxy-terminal domain of flagellin. *Nat Immunol* 9(10):1171-1178.

57. Bergsbaken T, Fink SL, & Cookson BT (2009) Pyroptosis: host cell death and inflammation. *Nat Rev Microbiol* 7(2):99-109.

58. Fink SL & Cookson BT (2006) Caspase-1-dependent pore formation during pyroptosis leads to osmotic lysis of infected host macrophages. *Cell Microbiol* 8(11):1812-1825.

59. Gomez-Valero L*, et al.* (2014) Comparative analyses of Legionella species identifies genetic features of strains causing Legionnaires' disease. *Genome Biol* 15(11):505.

60. Rolando M & Buchrieser C (2014) Legionella pneumophila type IV effectors hijack the transcription and translation machinery of the host cell. *Trends Cell Biol* 24(12):771-778.

61. Herrmann V*, et al.* (2011) GamA is a eukaryotic-like glucoamylase responsible for glycogen- and starch-degrading activity of Legionella pneumophila. *Int J Med Microbiol : IJMM* 301(2):133-139.

62. Gomez-Valero L*, et al.* (2011) Extensive recombination events and horizontal gene transfer shaped the Legionella pneumophila genomes. *BMC Genomics* 12:536.

63. Cazalet C*, et al.* (2004) Evidence in the Legionella pneumophila genome for exploitation of host cell functions and high genome plasticity. *Nat Genetics* 36(11):1165-1173.

64. Brown A, Vickers RM, Elder EM, Lema M, & Garrity GM (1982) Plasmid and surface antigen markers of endemic and epidemic Legionella pneumophila strains. *J Clin Microbiol* 16(2):230-235.

65. Cazalet C*, et al.* (2008) Multigenome analysis identifies a worldwide distributed epidemic Legionella pneumophila clone that emerged within a highly diverse species. *Genome Res* 18(3):431-441.

66. Bandyopadhyay P, Liu S, Gabbai CB, Venitelli Z, & Steinman HM (2007) Environmental mimics and the Lvh type IVA secretion system contribute to virulence-related phenotypes of *Legionella pneumophila*. *Infect Immun* 75(2):723-735.

67. Chien M*, et al.* (2004) The genomic sequence of the accidental pathogen Legionella pneumophila. *Science* 305(5692):1966-1968.

68. Brassinga AKC*, et al.* (2003) A 65-Kilobase Pathogenicity Island Is Unique to Philadelphia-1 Strains of *Legionella pneumophila*. *J Bacteriol* 185(15):4630-4637.

69. Glockner G*, et al.* (2008) Identification and characterization of a new conjugation/type IVA secretion system (trb/tra) of Legionella pneumophila Corby localized on two mobile genomic islands. *Int J Med Microbiol* 298(5-6):411-428.

70. Lautner M, Schunder E, Herrmann V, & Heuner K (2013) Regulation, integrase-dependent excision, and horizontal transfer of genomic islands in Legionella pneumophila. *J Bacteriol* 195(7):1583-1597.

71. Feely J*, et al.* (1979) Charcoal-yeast extract agar: primary isolation medium for Legionella pneumophila. *J Clin Microbiol* 10(4):437-441.

72. Bryan A, Harada K, & Swanson MS (2011) Efficient generation of unmarked deletions in Legionella pneumophila. *Appl Env Microbiol* 77(7):2545-2548.

73. Vogel JP (1998) Conjugative Transfer by the Virulence System of Legionella pneumophila. *Science* 279(5352):873-876.

74. Doleans-Jordheim A*, et al.* (2006) Growth-phase-dependent mobility of the lvh-encoding region in Legionella pneumophila strain Paris. *Microbiology* 152(Pt 12):3561-3568.

75. Swanson MS & Isberg RR (1995) Association of Legionella pneumophila with the macrophage endoplasmic reticulum *Infect Immun* 63(9):3609-3620.

76. Goldberg M, Belkowski LS, & Bloom BR (1990) Regulation of macrophage function by interferon-gamma. Somatic cell genetic approaches in murine macrophage cell lines to mechanisms of growth inhibition, the oxidative burst, and expression of the chronic granulomatous disease gene. *J Clin Invest* 85(2):563-569.

77. Rao C, Benhabib H, & Ensminger A (2013) Phylogenetic Recostruction of the *Legionella pneumophila* Philadelphia-1 Laboratory Strains through Comparative Genomics. *PloS One* 8(5).

78. Williams KP (2002) Integration sites for genetic elements in prokaryotic tRNA and tmRNA genes: sublocation preference of integrase subfamilies. *Nucleic Acids Res* 30(4):866-875.

79. Kohanski MA, Dwyer DJ, Hayete B, Lawrence CA, & Collins JJ (2007) A common mechanism of cellular death induced by bactericidal antibiotics. *Cell* 130(5):797-810.

80. Storey MV, Langmark J, Ashbolt NJ, & Stenstrom TA (2004) The fate of legionellae within distribution pipe biofilms: Measurement of their persistence, inactivation and detachment. *Water Sci Technol* 49(11-12):269-275.

81. Klebanoff SJ (2005) Myeloperoxidase: friend and foe. *J Leuk Biol* 77(5):598-625.

82. Wright E*, et al.* (2003) *Naip5* Affects Host Susceptibility to the Intracellular Pathogen *Legionella pneumophila*. *Curr Biol* 13(1):27-36.

83. Ren T, Zamboni D, Roy C, Dietrich W, & Vance R (2006) Flagellin-Deficient *Legionella* Mutants Evade Caspase-1- and *Naip5*-Mediated Macrophage Immunity *PLoS Pathogens* 2(3).

84. Muder RR, Yu VL, & Woo AH (1986) Mode of Transmission of Legionella pneumophila. *Arch Intern Med* 146(8):1607-1612.

85. Arambula D*, et al.* (2013) Surface display of a massively variable lipoprotein by a *Legionella* diversity-generating retroelement. *Proc Natl Acad Sci USA* 110(20):8212-8217.

86. Singh VK, Moskovitz J, Wilkinson B, & Jayaswal R (2001) Molecular characterization of a chromosomal locus in *Staphylococcus aureus* that contributes to oxidative defence and is highly induced by the cell-wall-active antibiotic oxacillin. *Microbiology* 147:3037-3045.

87. Moskovitz J*, et al.* (1995) *Escherichia coli* Peptide Methionine Sulfoxide Reductase Gene: Regulation of Expression and Role in Protecting Against Oxidative Damage. *J Bacteriol* 177(3):502-507.

88. Douglas T, Daniel DS, Parida BK, Jagannath C, & Dhandayuthapani S (2004) Methionine sulfoxide reductase A (MsrA) deficiency affects the survival of Mycobacterium smegmatis within macrophages. *J Bacteriol* 186(11):3590-3598.

89. Hebrard M, Viala JP, Meresse S, Barras F, & Aussel L (2009) Redundant hydrogen peroxide scavengers contribute to Salmonella virulence and oxidative stress resistance. *J Bacteriol* 191(14):4605-4614.

90. Murga R*, et al.* (2001) Role of biofilms in the survival of *Legionella pneumophila* in a model potable-water system. *Microbiology* 147:3121-3126.

91. Buse HY & Ashbolt NJ (2011) Differential growth of *Legionella pneumophila* strains within a range of amoebae at various temperatures associated with in-premise plumbing. *Lett. Appl. Microbiol* 53(2):217-224.

92. Tyson JY*, et al.* (2013) Multiple *Legionella pneumophila* type II secretion substrates, including a novel protein, contribute to differential infection of the amoebae *Acanthamoeba castellanii, Hartmonella vermiformis* and *Naegleria lovaniensis*. *Infect Immun* 81(5):1399-1410.

93. Buse HY, Schoen ME, & Ashbolt NJ (2012) Legionellae in engineered systems and use of quantitative microbial risk assessment to predict exposure. *Water Res* 46(4):921-933.

94. Lin Y, Stout JE, & Yu VL (2011) Controlling *Legionella* in Hospital Drinking Water: An Evidence-Based Review of Disinfection Methods. *Infect Contr Hosp Epidemiol* 32(2):166-173.

95. Gray MJ, Wholey WY, & Jakob U (2013) Bacterial responses to reactive chlorine species. *Ann Rev Microbiol* 67:141-160.

96. Slauch JM (2011) How does the oxidative burst of macrophages kill bacteria? Still an open question. *Mol Microbiol* 80(3):580-583.

97. Flynn KJ & Swanson MS (2014) Integrative conjugative element ICE-betaox confers oxidative stress resistance to Legionella pneumophila in vitro and in macrophages. *mBio* 5(3):e01091-01014.

98. Koraimann G & Wagner MA (2014) Social behavior and decision making in bacterial conjugation. *Front Cell Infect Microbiol* 4:54.

99. Rodriguez-Blanco A, Lemos ML, & Osorio CR (2012) Integrating conjugative elements as vectors of antibiotic, mercury, and quaternary ammonium compound resistance in marine aquaculture environments. *Antimicrob Agents Chemo* 56(5):2619-2626.

100. Frost LS & Koraimann G (2010) Regulation of bacterial conjugation: balancing opportunity with adversity. *Future Microbiol* 5(7):1057-1071.

101. Stone BJ & Abu Kwaik Y (1998) Expression of multiple pili by Legionella pneumophila: identification and characterization of a type IV pilin gene and its role in adherence to mammalian and protozoan cells. *Infect Immun* 66(4):1768-1775.

102. Segal G & Shuman HA (1998) Intracellular multiplication and human macrophage killing by Legionella pneumophila are inhibited by conjugal components of IncQ plasmid RSF1010. *Mol Microbiol* 30(1):197-208.

103. Beaber JW, Hochhut B, & Waldor MK (2004) SOS response promotes horizontal dissemination of antibiotic resistance genes. *Nature* 427(6969):72-74.

104. Sentchilo V, Ravatn R, Werlen C, Zehnder AJ, & van der Meer JR (2003) Unusual integrase gene expression on the clc genomic island in Pseudomonas sp. strain B13. *J Bacteriol* 185(15):4530-4538.

105. Wang Y, Shoemaker NB, & Salyers AA (2004) Regulation of a Bacteroides operon that controls excision and transfer of the conjugative transposon CTnDOT. *J Bacteriol* 186(9):2548-2557.

106. Bose B & Grossman AD (2011) Regulation of horizontal gene transfer in Bacillus subtilis by activation of a conserved site-specific protease. *J Bacteriol* 193(1):22-29.

107. Clewell DB (2011) Tales of conjugation and sex pheromones: A plasmid and enterococcal odyssey. *Mobile Gene Elements* 1(1):38-54.

108. Haudecoeur E & Faure D (2010) A fine control of quorum-sensing communication in Agrobacterium tumefaciens. *Commun Integr Biol* 3(2):84-88.

109. Rao C, Benhabib H, & Ensminger AW (2013) Phylogenetic reconstruction of the Legionella pneumophila Philadelphia-1 laboratory strains through comparative genomics. *PLoS One* 8(5):e64129.

110. Molofsky AB & Swanson MS (2003) Legionella pneumophila CsrA is a pivotal repressor of transmission traits and activator of replication. *Mol Microbiol* 50(2):445-461.

111. Nevo O, Zusman T, Rasis M, Lifshitz Z, & Segal G (2014) Identification of Legionella pneumophila effectors regulated by the LetAS-RsmYZ-CsrA regulatory cascade, many of which modulate vesicular trafficking. *J Bacteriol* 196(3):681-692.

112. Marden JN*, et al.* (2013) An unusual CsrA family member operates in series with RsmA to amplify posttranscriptional responses in Pseudomonas aeruginosa. *Proc Nat Acad USA* 110(37):15055-15060.

113. O'Connor TJ, Adepoju Y, Boyd D, & Isberg RR (2011) Minimization of the Legionella pneumophila genome reveals chromosomal regions involved in host range expansion. *Proc Nat Acad USA* 108(36):14733-14740.

114. Feeley JC*, et al.* (1979) Charcoal-yeast extract agar: primary isolation medium for Legionella pneumophila. *J Clin Microbiol* 10(4):437-441.

115. Larkin MA*, et al.* (2007) Clustal W and Clustal X version 2.0. *Bioinformatics* 23(21):2947-2948.

116. Guindon S*, et al.* (2010) New algorithms and methods to estimate maximum-likelihood phylogenies: assessing the performance of PhyML 3.0. *System Biol* 59(3):307-321.

117. Letunic I & Bork P (2011) Interactive Tree Of Life v2: online annotation and display of phylogenetic trees made easy. *Nucleic Acids Res* 39(Web Server issue):W475-478.

118. Sullivan MJ, Petty NK, & Beatson SA (2011) Easyfig: a genome comparison visualizer. *Bioinformatics* 27(7):1009-1010.

119. Berger KH & Isberg RR (1993) Two distinct defects in intracellular growth complemented by a single genetic locus in Legionella pneumophila. *Mol Microbiol* 7(1):7-19.

120. Wiater LA, Sadosky AB, & Shuman HA (1994) Mutagenesis of Legionella pneumophila using Tn903 dlllacZ: identification of a growth-phase-regulated pigmentation gene. *Mol Microbiol* 11(4):641-653.

121. Mukherjee S*, et al.* (2011) CsrA-FliW interaction governs flagellin homeostasis and a checkpoint on flagellar morphogenesis in Bacillus subtilis. *Mol Microbiol* 82(2):447-461.

122. Mukherjee S*, et al.* (2015) Adaptor-mediated Lon proteolysis restricts Bacillus subtilis hyperflagellation. *Proc Natl Acad Sci U S A* 112(1):250-255.

123. Swanson MS & Isberg RR (1996) Identification of Legionella pneumophila mutants that have aberrant intracellular fates. *Infect Immun* 64(7):2585-2594.

124. Goldberg M, Belkowski LS, & Bloom BR (1990) Regulation of macrophage function by interferon-gamma. Somatic cell genetic approaches in murine macrophage cell lines to mechanisms of growth inhibition, the oxidative burst, and expression of the chronic granulomatous disease gene. *J Clin Invest* 85(2):563-569.

125. Vogel JP, Andrews HL, Wong SK, & Isberg RR (1998) Conjugative transfer by the virulence system of Legionella pneumophila. *Science* 279(5352):873-876.

126. Gibson DG*, et al.* (2009) Enzymatic assembly of DNA molecules up to several hundred kilobases. *Nature Meth* 6(5):343-345.

127. Yasbin RE & Young FE (1974) Transduction in Bacillus subtilis by bacteriophage SPP1. *J Virol* 14(6):1343-1348.

128. Wee BA, Woolfit M, Beatson SA, & Petty NK (2013) A distinct and divergent lineage of genomic island-associated Type IV Secretion Systems in Legionella. *PLoS One* 8(12):e82221.

129. Segal G, Russo JJ, & Shuman HA (1999) Relationships between a new type IV secretion system and the icm/dot virulence system of Legionella pneumophila. *Mol Microbiol* 34(4):799-809.

130. Ilangovan A, Connery S, & Waksman G (2015) Structural biology of the Gram-negative bacterial conjugation systems. *Trends Microbiol*.

131. Waldor MK (2010) Mobilizable genomic islands: going mobile with oriT mimicry. *Mol Microbiol* 78(3):537-540.

132. MacMillan F, Budiman K, Angerer H, & Michel H (2006) The role of tryptophan 272 in the Paracoccus denitrificans cytochrome c oxidase. *FEBS Lett* 580(5):1345-1349.

133. Moskovitz J*, et al.* (1995) Escherichia coli peptide methionine sulfoxide reductase gene: regulation of expression and role in protecting against oxidative damage. *J Bacteriol* 177(3):502-507.

134. Berger KH, Merriam JJ, & Isberg RR (1994) Altered intracellular targeting properties associated with mutations in the Legionella pneumophila dotA gene. *Mol Microbiol* 14(4):809-822.

135. Molofsky AB, Shetron-Rama LM, & Swanson MS (2005) Components of the Legionella pneumophila flagellar regulon contribute to multiple virulence traits, including lysosome avoidance and macrophage death. *Infect Immun* 73(9):5720-5734.

136. Rasis M & Segal G (2009) The LetA-RsmYZ-CsrA regulatory cascade, together with RpoS and PmrA, post-transcriptionally regulates stationary phase activation of Legionella pneumophila Icm/Dot effectors. *Mol Microbiol* 72(4):995-1010.

137. Miyamoto H, Yoshida S, Taniguchi H, & Shuman HA (2003) Virulence conversion of Legionella pneumophila by conjugal transfer of chromosomal DNA. *J Bacteriol* 185(22):6712-6718.

138. Dubey AK, Baker CS, Romeo T, & Babitzke P (2005) RNA sequence and secondary structure participate in high-affinity CsrA-RNA interaction. *RNA* 11(10):1579-1587.

139. Duss O, Michel E, Diarra dit Konte N, Schubert M, & Allain FH (2014) Molecular basis for the wide range of affinity found in Csr/Rsm protein-RNA recognition. *Nucleic Acids Res* 42(8):5332-5346.

140. Mercante J, Edwards AN, Dubey AK, Babitzke P, & Romeo T (2009) Molecular geometry of CsrA (RsmA) binding to RNA and its implications for regulated expression. *J Molec Biol* 392(2):511-528.

141. Qin T*, et al.* (2009) Conjugative plasmid pLD-TEX-KL promotes growth of host bacterium Legionella dumoffii at low temperatures. *Arch Microbiol* 191(6):543-551.

142. Garduno RA, Garduno E, Hiltz M, & Hoffman PS (2002) Intracellular growth of Legionella pneumophila gives rise to a differentiated form dissimilar to stationary-phase forms. *Infect Immun* 70(11):6273-6283.

143. Hiltz MF*, et al.* (2004) Expression of magA in Legionella pneumophila Philadelphia-1 Is Developmentally Regulated and a Marker of Formation of Mature Intracellular Forms. *J Bacteriol* 186(10):3038-3045.

144. Saenkham P, Vattanaviboon P, & Mongkolsuk S (2009) Mutation in sco affects cytochrome c assembly and alters oxidative stress resistance in Agrobacterium tumefaciens. *FEMS Microbiol Lett* 293(1):122-129.

145. Li XZ, Livermore DM, & Nikaido H (1994) Role of efflux pump(s) in intrinsic resistance of Pseudomonas aeruginosa: resistance to tetracycline, chloramphenicol, and norfloxacin. *Antimicrob Agents Chemotherapy* 38(8):1732-1741.

146. Wilke MS, Lovering AL, & Strynadka NC (2005) Beta-lactam antibiotic resistance: a current structural perspective. *Curr Opinion Microbiol* 8(5):525-533.

147. Butala M, Zgur-Bertok D, & Busby SJ (2009) The bacterial LexA transcriptional repressor. *Cell Mol Life Sci* 66(1):82-93.

148. Andersson DI & Hughes D (2014) Microbiological effects of sublethal levels of antibiotics. *Nature Rev Microbiol* 12(7):465-478.

149. Goranov AI, Kuester-Schoeck E, Wang JD, & Grossman AD (2006) Characterization of the global transcriptional responses to different types of DNA damage and disruption of replication in Bacillus subtilis. *J Bacteriol* 188(15):5595-5605.

150. Auchtung JM, Lee CA, Monson RE, Lehman AP, & Grossman AD (2005) Regulation of a Bacillus subtilis mobile genetic element by intercellular signaling and the global DNA damage response. *Proc Nat Acad Sci USA* 102(35):12554-12559.

151. Baharoglu Z, Bikard D, & Mazel D (2010) Conjugative DNA transfer induces the bacterial SOS response and promotes antibiotic resistance development through integron activation. *PLoS Genetics* 6(10):e1001165.

152. Charpentier X, Kay E, Schneider D, & Shuman HA (2011) Antibiotics and UV radiation induce competence for natural transformation in Legionella pneumophila. *J Bacteriol* 193(5):1114-1121.

153. Ambur OH*, et al.* (2009) Genome dynamics in major bacterial pathogens. *FEMS Microbiol Rev* 33(3):453-470.

154. Marra A & Shuman HA (1992) Genetics of Legionella pneumophila virulence. *Ann Rev Genetics* 26:51-69.

155. Sahr T*, et al.* (2009) Two small ncRNAs jointly govern virulence and transmission in Legionella pneumophila. *Mol Microbiol* 72(3):741-762.

156. Weissenmayer BA, Prendergast JG, Lohan AJ, & Loftus BJ (2011) Sequencing illustrates the transcriptional response of Legionella pneumophila during infection and identifies seventy novel small non-coding RNAs. *PloS One* 6(3):e17570.

157. Jayakumar D, Early JV, & Steinman HM (2012) Virulence phenotypes of Legionella pneumophila associated with noncoding RNA lpr0035. *Infect Immun* 80(12):4143-4153.